JRC Scientific and Technical Reports

Multimedia assessment of pollutant pathways in the environment: a Global scale model

A. Pistocchi, D. Marinov, S. Pontes, G. Zulian, M. Trombetti

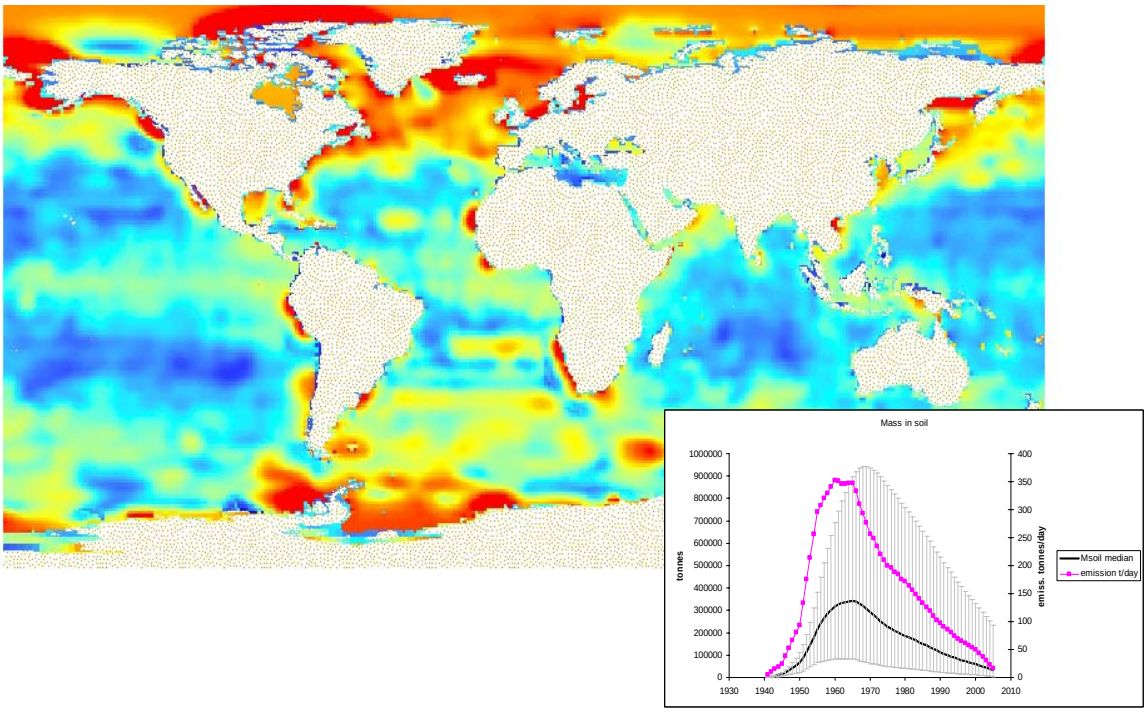

EUR 24911 EN - 2011

JRC EUROPEAN COMMISSION

ies Institute for Environment and Sustainability

The mission of the JRC-IES is to provide scientific-technical support to the European Union's policies for the protection and sustainable development of the European and global environment.

European Commission
Joint Research Centre
Institute for Environment and Sustainability

Contact information
Address: Dimitar Marinov, JRC, IES, TP 460, Via E. Fermi 2749, 21027 Ispra (VA), Italy
E-mail: dimitar.marinov@jrc.ec.europa.eu
Tel.: +39 0332 783630
Fax: +39 0332 785601

http://ies.jrc.ec.europa.eu/
http://www.jrc.ec.europa.eu/

JRC 65989

EUR 24911 EN

ISBN 978-92-79-20921-5 (print)
ISBN 978-92-79-20922-2 (pdf)

ISSN 1018-5593 (print)
ISSN 1831-9424 (online)

doi: 10.2788/47157

Luxembourg: Publications Office of the European Union

Printed in Italy

Executive summary

The report describes the assumptions, equations and a few examples of preliminary applications of a global spatialized steady-state box model entitled Multimedia Assessment of Pollutant Pathways in the Environment (MAPPE-Global). The model grounds on the concept of already developed European version of MAPPE chemical fate model (Pistocchi, 2008; Pistocchi et al., 2010a; and Pistocchi et al., 2010b).

MAPPE-Global computes the removal rates of a substance with given physical-chemical properties in an evaluative environment for the entire world with a resolution of 1^{o}x1^{o} considering atmospheric boundary layer, land (natural and agriculture soils, forests, impervious surfaces, frozen territories), surface water (including lakes, inland wetlands and reservoirs) and oceans and seas.

The model is able to consider chemical emissions in one or more of the environmental compartments and estimates chemical concentrations and fluxes accounting in general the following types of chemical fate processes: partitioning (gas, liquid or solid), degradation, advective transport, diffusive transport, and transport to a "sink" represented by deep ocean layers.

In MAPPE-Global the chemical degradation may occur in air, land and water and may be due to a number of biological, physical or chemical processes such as photolysis, hydrolysis, chemical and biological transformation. The model assumes that chemical degradation follows a simple linear law and sufficiently well described by a chemical half-life.

The advective transport to other compartments, in the model, may be distinguished in "vertical" and "horizontal" processes. The former includes transfer between compartments of the same cell: wet and dry deposition from the atmosphere to land and oceans; discharges of water from land to oceans. The latter considers the transfer outside of the cell: runoff fluxes from soil to the stream network; wind advection from the atmospheric boundary layer of one cell to the surrounding cells; and ocean current advection from one cell to the surrounding cells.

The diffusive transport is essentially gas absorption from the atmosphere to surfaces (land and ocean), and volatilization from land and ocean. No dispersive or diffusive horizontal transport between cells is considered in MAPPE-Global.

The transport to the deep ocean "sink" through particle settling may be assimilated to "vertical" advective transfer according to MAPPE-Global assumptions.

At this stage, MAPPE Global does not explicitly compute chemical transport in space, but only the fate of a substance at each location in space. However, the model computes for each grid cell the mass fluxes of chemical that are available for transformation inside or for transport outside of the cell, in addition to concentrations from local emissions. Therefore, MAPPE Global is developed specifically to respond questions as:

- How will a chemical spread across different media in the different climatic and landscape settings?
- How important is the variability of environmental processes in determining the fate of chemicals across the globe?

In addition, the model enables estimating, for virtually any location in the world, representative parameters of the environmental removal rates that determine the fate of a given contaminant. These rates may be used to feed a zero-dimensional (lumped) time-dependent model that allows computing "environmental breakthrough curves", hence to forecast which will be the main receptors of the chemical emissions, and consequently, the most likely areas where ecological and human health impacts would be expected.

In order to evaluate the performance of the MAPPE-Global model a comparison with established models, such as Impact World (Shaked et al., 2008) and USEtox (Rosenbaum et al., 2008), was made. Keeping in mind the limitations of MAPPE-Global as well as specific features of the other models (e.g. accounting of advection, spatial resolution, etc.) the comparison covered only crosschecking of the intermedia removal rate coefficients.

In general, MAPPE Global underestimates the air transfer to the other environmental compartments, apart from the convey to oceans/seas, which is overrated. A correlation of R^2=0.18 between MAPPE-Global and Impact World is found when comparing the transfer from soil to fresh water (MAPPE undervalued Impact World), while the USEtox forecasts are about 9-10 times less in contrast to MAPPE ones. Oppositely, MAPPE Global underestimates the export from soil to atmosphere by one order of magnitude in distinction to USEtox and by 2 orders comparatively to Impact World. The estimates of MAPPE-Global for the exchange between ocean and atmosphere are higher 2 and 5 times in comparison with results of USEtox and Impact World, respectively.

Additionally, the impact of ambient temperature, in terms of the variability of the air-water partition coefficient and degradation, on the removal rates is also studied. The test performed for Lindane demonstrated that for multimedia chemicals the impact seems to be low because the medians and the range of variability of results with and without accounting temperature are quite similar.

Then, aiming to study the spatial differentiation of environmental fate of different chemicals a "test set" of 34 organic substances is adopted. The set comprises chemicals having a large diversity of physical chemical properties in order to be representative, as far as possible, and also to reveal the potential differences in their environmental behaviour.

The MAPPE-Global model results showed that for the case of air no advection the range of variability is 1-4 orders of magnitude and it is driven by the gas exchange and/or wet deposition. However, when the degradation rate is low comparing to gas exchange, the variability of total air removal rates is higher and vice versa. Thus, could be concluded that for persistent chemicals the degradation, as an elimination process, regulates (eventually reducing) the range of variability of total air removal rates, which changeability is primarily associated with the wide spatial fluctuations of gas exchange or wet deposition at global scale. This conclusion is even more strongly valid when the advection is accounted.

In addition, it was found that the variability of the total removal rates in soil for all chemicals considered remains below 2.5 orders of magnitude but for 68% of the chemical groups the variability is not exceeding more than one order of extent.

Nonetheless, this is not the case for the ocean compartment (no advection case) since a few chemical groups in practice show no variability while for the rest ones the removal rates are highly variable.

Moreover, it was confirmed again the role of degradation and advection (when considered) as controlling factors of the total removal rates for the soil and ocean compartments.

Besides, the surface water compartment shows rather homogeneous behavior for all chemical groups with variability up to 1.5 orders of magnitude because of the specific assumptions (limitations) under which it was considered in the present version of the MAPPE Global model.

In order to identify the reason for variability and trying to answer whether or not the variability follows similar spatial patterns, distribution maps at global scale were calculated for all chemicals of the test-set. This allowed to identify the global fate patterns of flyers, swimmers, soil-bound and multimedia chemical substances.

Finally, the reports demonstrates how the maps of environmental removal rates, calculated by MAPPE-Global, could be further explored by a zero-dimensional time-dependent global model representing an alternative formulation of MAPPE model. As an example application, it was referred to the case of DDT, for which is found a good agreement with the model results of Schenker et al. (2008) providing the global DDT's trend in air, soil and ocean in the decade 1985-1995.

Contents

List of Figures

List of Tables

1. Introduction

The report describes the assumptions, equations and a few examples of preliminary results of a global spatialized box model entitled Multimedia Assessment of Pollutant Pathways in the Environment (MAPPE-Global). The model grounds on the concept of the recently developed MAPPE-Europe model for chemicals fate in the environment (Pistocchi, 2008; Pistocchi et al., 2010a; and Pistocchi et al., 2010b).

MAPPE-Global computes the removal rates of a substance with given physical-chemical properties in an evaluative environment for the whole world with a resolution of 1^{o}x1^{o} (except for some parameters, which are defined even at finer resolution). The environmental compartments considered are:

1) Atmospheric boundary layer
2) Land (soil, forests, impervious surfaces, frozen territories)
3) Stream network (including lakes, inland wetlands and reservoirs)
4) Ocean and seas.

The Figure 1 shows a scheme of the topology and connections between the different environmental compartments accounted by MAPPE-Global. The model is able to consider emissions of a chemical in one or more of the environmental compartments. From emissions, concentrations are computed in each compartment using the continuous stirred tank reactor (CSTR) scheme, except for the stream network where a plug flow (PF) scheme is adopted. The CSTR and PF schemes provide an estimate of concentrations by specifying four types of chemical fate processes, namely:

1) degradation
2) advective transport
3) diffusive transport
4) transport to a "sink" represented by deep ocean layers.

The chemical degradation may occur in air, land and water. It may be due to a number of biological, physical or chemical processes such as photolysis, hydrolysis, chemical and biological transformation. The model assumes that chemical degradation follows a simple linear law, i.e. it is sufficiently well described by a chemical half-life. The half-lives may spatially vary following a number of factors, such as pH, soil moisture, OH concentration, sun irradiance, and temperature. For simplicity, the present version of the model considers only the degradation dependence on temperature.

The advective transport to other compartments may be distinguished in "vertical" and "horizontal" processes.

The former includes transfer between compartments of the same cell:

- wet and dry deposition from the atmosphere to land and oceans
- discharges of water from land to oceans

The latter includes transfer to outside of the cell:

- runoff fluxes from soil to the stream network
- wind advection from the atmospheric boundary layer of one cell to the surrounding cells
- ocean current advection from one cell to the surrounding cells.

The "horizontal" processes are only considered when computing local concentrations from an isolated source and the associated mass fluxes which feed the transport of chemicals from the cell of emission

to the regional or global scale. However, the fluxes originated from neighboring cells are not considered when computing concentrations at a given cell.

The diffusive transport is essentially gas absorption from the atmosphere to surfaces (land and ocean), and volatilization from land and ocean. No dispersive or diffusive horizontal transport between cells is considered.

The transport to the deep ocean "sink" through particle settling may be assimilated to "vertical" advective transfer.

Each environmental compartment is structured in a complex organization of physical phases (gas, liquid, solid). Accordingly, the advective fluxes are in general composed of a solid, liquid and gas phase. Within each medium, a steady state is assumed so that concentrations between different phases are univocally related through appropriate partition coefficients. Moreover, the land compartment is simplistically distinguished in four categories, soil, impervious surfaces, water bodies and vegetation (forest, in turn divided in three sub-categories). The four categories are represented through the percentage by which each of them covers the $1^{o}x1^{o}$ cell surface area.

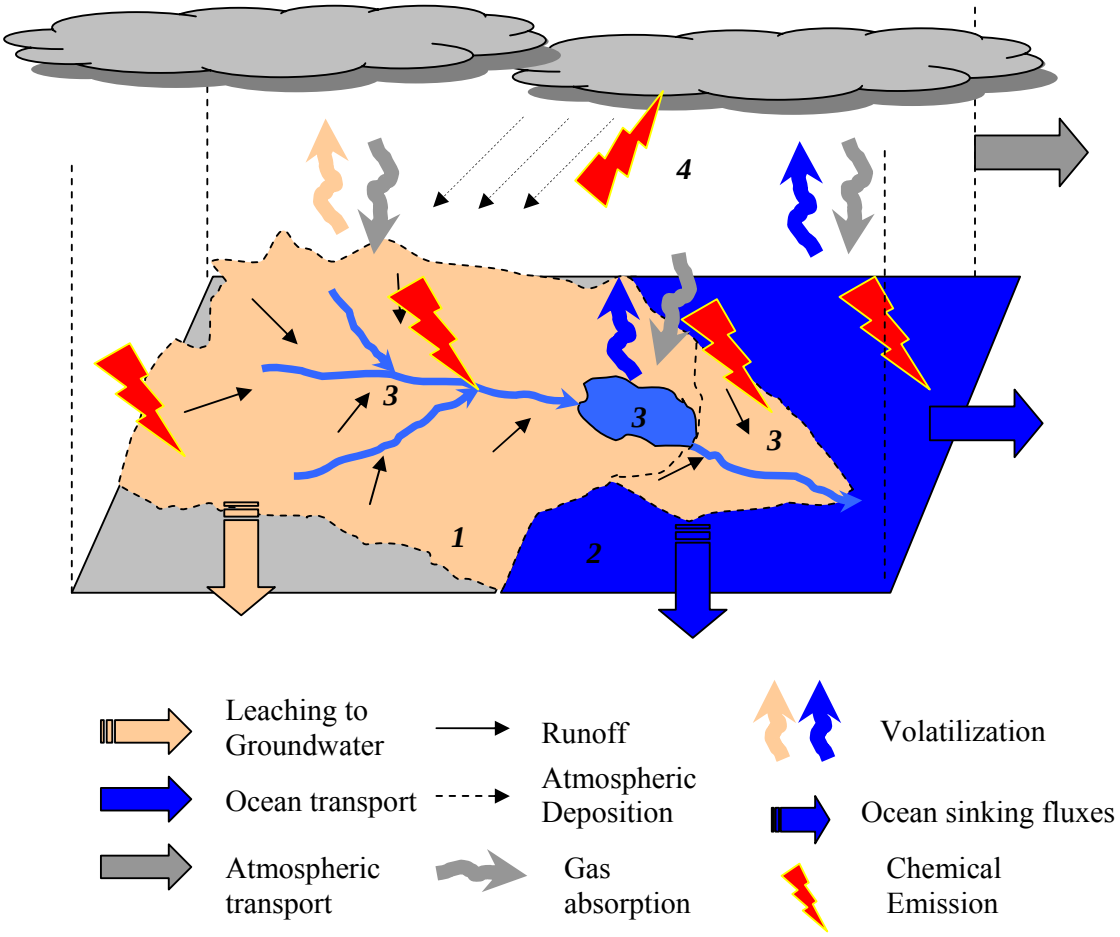

Figure 1 – conceptual scheme of the evaluative environment considered in MAPPE model.

At this stage, MAPPE Global does not explicitly compute chemical transport in space, but only the fate of a substance at each location in space. In order to assess the spatial pattern of contamination originated from spatially distributed emissions, a full transport model must be used. However, the model computes for each grid cell the mass fluxes of chemical that are available for transport outside of the cell, in addition to local concentrations from local emissions. Grounding on these features, the model can be only used when at least one of the following conditions is met:

1) emissions are uniform in space
2) effect of emissions away from the location they rise are not of interest.

MAPPE Global is developed specifically to respond questions concerning the environmental fate of contaminants taking into account the variability of environmental processes at the global scale. As such, the model can and should be used to quantify the changes of pollutant fate in response to spatial variability of emissions and chemical fate processes, such as:

- How will a chemical spread across different media in different climatic and landscape settings?
- How important is the variability of environmental processes in determining the fate of chemicals across the globe?
- How much of a chemical emitted to soil will result in a load to the atmosphere or waters?

In addition to the above questions, the model enables estimating, for virtually any location in the world, representative parameters of the environmental removal rates that determine the fate of a contaminant. These rates may be used to feed a zero-dimensional (lumped) time-dependent model of chemical mass balance that allows computing "environmental breakthrough curves" as will be discussed later in this report. The environmental breakthrough curves of a chemical enable decision makers to get a picture of how a given time series of chemical emissions will distribute in time among the different media (air, soil, water), hence to forecast which will be the main receptors of the chemical emissions, and consequently, the most likely areas where ecological and human health impacts will be expected.

2. Spatialized steady state global model

The MAPPE Global model computes chemical mass M_x (kg) for a certain grid cell as a algebraic combination of the maps of emissions E_x (kg/day) and removal rates K_x (day^{-1}) for each medium:

$$M_x = \frac{E_x}{K_x}$$

where x indicates air, soil, or ocean environment.

In a similar way, the mass fluxes of a given chemical L_x (kg/day) originated from a cell and available for a long range transport ("loads") are computed as:

$$L_x = M_x K_{adv,x}$$

where $Kadv,x$ (day^{-1}) are the maps of advection removal rates in different media, associated to wind in the atmosphere, ocean currents, or runoff and erosion from soils.

In the present version of the model the surface water is considered only as a "transit" compartment which transports the chemical load originated from land to the marine environment.

2.1 Atmospheric compartment

Aerosol partitioning

The mass fraction ϕ (-) of chemical that is in aerosol phase is computed as:

$$\phi = \frac{10^{-2.91} K_{oa} OC}{1 + 10^{-2.91} K_{oa} OC}$$

where K_{oa} (-) is the chemical octanol-air partition coefficient, usually set to K_{ow}/K_{aw} while OC (kg m^{-3}) is the concentration of particulate organic carbon in the atmosphere. Respectively, the K_{ow} (-) is the octanol-water partitioning coefficient and K_{aw} (-) is the air-water partitioning coefficient (non-dimensional Henry's constant). The latter is calculated depending of the atmospheric temperature T *(K)* as:

$$K_{aw} = K_{aw_0} \exp(\gamma T)$$

where K_{aw_0} (-) is the air-water partitioning coefficient at reference temperature and γ (-) is the temperature-degradation coefficient.

Wet deposition

The wet deposition velocity K_{wet} (m s^{-1}) is computed from the annual average precipitation rate P (m day^{-1}) as:

$$K_{wet} = (S\phi + \frac{1}{K_{aw}}(1-\phi))\frac{P}{86400}$$

where S (-) is a scavenging factor usually set to $2*10^5$.

Particle dry deposition

The particle deposition velocity K_{part} (m s^{-1}) is computed from OC and the deposition flux of atmospheric particulate organic carbon F_{OC} (kg m^{-2} s^{-1}), as:

$$K_{part} = \phi \frac{F_{OC}}{OC}.$$

Gas absorption

The absorption velocity of atmospheric chemicals in gas phase depends on the type of ground surface.

The following categories of ground surface are presently considered in the model:

- agricultural or natural (bare) soil
- impervious surface (urban, sealed soil, etc.)
- desert or permanently frozen soil
- forest deciduous
- forest evergreen (broadleaves or conifers)
- water (lakes, reservoirs and rivers; oceans and seas).

Conventionally, the following absorption velocities are given for the three types of forest:

- deciduous: $v_{f,d} = 0.036$ m s^{-1}
- evergreen, broadleaved: $v_{f,b} = 0.072$ m s^{-1}
- evergreen, conifers: $v_{f,c} = 0.0078$ m s^{-1}

The above values are taken from MacLachlan and Horstmann (1998), as measured velocities on oaks (0.036 m s^{-1}) and spruce (0.0078 m s^{-1}) in Germany; in the case of evergreen broadleaved forest it is assumed that the speed is ca. 50% higher than the one for oaks. These velocities are referred to chemicals such as dioxins or polychlorobyphenils, having a molecular weight of about 300 g mol^{-1}, and need to be rescaled for other chemicals.

Therefore, the absorption velocity on forest areas, $K_{gas,\ forest}$ (m s^{-1}) is specified as:

$$K_{gas,forest} = \left(0.036\frac{Dec}{100} + 0.0078\ \frac{Eve}{100}(1 - \frac{Bro}{100}) + 0.054\frac{Eve}{100}\frac{Bro}{100}\right)\left(\frac{300}{MW}\right)^{0.5}$$

where *Dec* is the percentage of deciduous forest cover, *Eve* is the percentage of evergreen forest, and *Bro* is the percentage of broadleaved forest.

The absorption velocity on soils, $K_{gas,\ soil}$ (m s^{-1}) is evaluated using a two-layer resistance model (Pistocchi, 2005):

$$K_{gas,soil} = \frac{D_a}{(\xi h_s + d_a)}$$

where h_s = 0.15 m is half of the soil layer thickness (set to 0.3m), ξ (-) is the tortuosity factor $\xi = \frac{\omega^{2/3}}{(\omega - \theta)^2}$; ω (-) and θ (-) are soil porosity and soil water content, d_a is the thickness of the laminar microlayer at the air-soil interface (which is assumed to be negligible compared to ξh), and D_a is the diffusion coefficient of the chemical in air (m^2 s^{-1}).

Then, assuming constant values for both porosity, set to 0.4, and soil water content, set to 0.2, the tortuosity coefficient simply equals to 13.6. The diffusion coefficient in air (m^2/s) can be estimated as Schwarzenbach et al., (1993):

$$D_a = 0.000025 \cdot \left(\frac{18}{MW}\right)^{0.5}$$

where 0.000025 m^2/s is the diffusion coefficient of H_2O in air.

Under these assumptions, $K_{gas,\ soil}$ (m s^{-1}) becomes

$$K_{gas,\ soil} = 0.0000123 \cdot \left(\frac{18}{MW}\right)^{0.5}$$

On impervious surfaces (e.g. urban, sealed soils) it is assumed that no absorption occurs. The same assumption was applied to deserts or permanently frozen land.

On water, the velocity of absorption $K_{gas,\ water}$ (m s^{-1}) is evaluated using a two resistance model (see Pistocchi, 2005 for details) in the form:

$$K_{gas,water} = \frac{v_a v_w}{v_a K_{aw} + v_w}$$

where v_a and v_w are the diffusion velocities (m s-1) in air and water, given by:

$$v_a = \left(\frac{18}{MW}\right)^{0.335}\left(0.002 \cdot u_{10} + 0.003\right)$$

$$v_w = \left(\frac{32}{MW}\right)^{0.285} \cdot \left(0.0000004 \cdot u_{10}^2 + 0.000004\right)$$

As a result, for each grid cell in the model, the gas absorption from atmosphere K_{gas} (m s^{-1}) is calculated as:

$$K_{gas} = K_{gas,water}\frac{w}{100} + \left(K_{gas,\ forest}\frac{Dec + Eve}{100} + K_{gas,\ soil}\left(1 - \frac{Dec + Eve}{100}\right)\right)\left(1 - \frac{Imp}{100}\right)\left(1 - \frac{w}{100}\right)$$

where w is the percentage of the cell that is water, and Imp the percentage that is impervious surface. Additionally, the spatial coverage of $K_{gas,forest}$ and $K_{gas,soil}$ respects the presence of the deserts or permanently frozen soils assuming there a zero value.

Degradation

The degradation processes in the atmosphere are specified by the degradation rate $K_{deg,a}$ (s^{-1}) as follows:

$$K_{\mathrm{deg},a} = \alpha_a \exp(\beta_a T)$$

where α_a (s^{-1}) and β_a (K^{-1}) are the degradation coefficients and temperature T is given in Kelvin degrees.

Total atmospheric removal rate

The total atmospheric removal rate K_{air} (d^{-1}) is:

$$K_{air} = 3600 \cdot \left(\frac{(K_{part} + (1-\phi)K_{gas} + K_{wet})}{ABL} + K_{\mathrm{deg},a} + \frac{u_{10}}{X} \right) \cdot 24$$

where ABL (m) is the height of the atmospheric boundary layer while the last term represents the air intramedium transport or dilution by the wind advection. Here u_{10} (m s^{-1}) is the wind speed at *10*m height and X (m) is the size of the calculation cells (approximately *100000* m corresponding to 1 degree resolution). Then, the term of advection rate quantifies the fraction of the air to be moved out through the lateral borders of the computational cells with u_{10} speed.

In the expression for K_{air}, the term for advection should be considered only for a single isolated emission which is an ideal extreme case.

The other extreme case is the situation when emissions occur in a uniform (homogeneous) way around the Globe, thus, the advection may be neglected. In this case, one should consider K'_{air} no advection:

$$K'_{air} = 3600 \cdot \left(\frac{(K_{part} + (1-\phi)K_{gas} + K_{wet})}{ABL} + K_{\mathrm{deg},a} \right) \cdot 24 .$$

Obviously, the real situations should be in between these two extremes.

Deposition

Atmospheric deposition rate Dep (d^{-1}) is the fraction of the atmospheric removal rate in a cell, which quantifies the air intermedia transfer and is computed as:

$$Dep = 3600 \cdot \frac{(K_{part} + (1-\phi)K_{gas} + K_{wet})}{ABL} \cdot 24$$

At this end worth mentioning that similarly to the other multimedia box models the atmospheric part of MAPPE Global does not distinguish wind directions. This limitation is likely to underestimate the role of long range transport on the fate and impact of the persistent chemicals. However, a further improvement of the air compartment of the model is foreseen in terms of an incorporation of an atmospheric source-receptor matrix, allowing to calculate the contaminant air concentration at a certain location as a sum of the contributions from local and remote emission sources, as done for example in the European version of MAPPE model (Pistocchi et al., 2008).

2.2 Soil compartment

Partitioning

In soil the chemical mass fractions in liquid R_{liq} (-) and solid R_{sol} (-) phases are computed as:

$$R_{liq} = \frac{\theta}{(K_d\ \rho + \theta + (\omega - \theta)K_{aw})}$$

$$R_{sol} = \frac{K_d\ \rho}{(K_d\ \rho + \theta + (\omega - \theta)K_{aw})}$$

where ω (-) and θ (-) are soil porosity and water content, ρ (kg l^{-1}) is the soil bulk density, and K_d (l kg^{-1}) is the chemical solid-liquid distribution coefficient. We assume constant values of porosity, set to *0.4*, and soil water content, set to *0.2*, as well as soil bulk density, set to *1.4* (kg l^{-1}). In addition, the spatial coverage of R_{liq} and R_{sol} respects the presence of the deserts or permanently frozen soils assuming there a zero value.

The chemical solid-liquid distribution coefficient is estimated as:

$K_d = 0.41\ OC_s\ K_{ow}$

where OC_s (l kg^{-1}) is the organic carbon content of soils.

Erosion

The K_{er} erosion rate (m s^{-1}) is estimated as:

$$K_{er} = 0.001\frac{SSY\ \cdot R_{sol}}{\rho} = 0.001\frac{SSY\ \cdot R_{liq}\ \cdot K_d}{\theta}$$

where *SSY* (kg m^{-2} s^{-1}) is the specific sediment yield and *0.001* is a conversion coefficient.

Volatilization

The volatilization rate K_{vl} (m s^{-1}) is:

$$K_{vl} = K_{aw}\ K_{gas,\ soil}\ \frac{R_{liq}}{\theta}$$

where $K_{gas,\ soil}$ was explained with reference to the air compartment.

The same formulas have been applied to the other types of land surfaces used in the model but accounting for their specific properties (for example substituting $K_{gas,\ soil}$ with $K_{gas,\ forest}$ in the formula for volatilization).

Runoff

The runoff rate K_Q (m d^{-1}) is meant here to include all removal mechanisms through water flows at the catchment scale, i.e. leaching to groundwater and direct runoff to surface water bodies; a further separation between these two mechanisms can be done on the basis of more refined data presently not available for the global scale. In the long term, as all recharge to groundwater is assumed to return to the rivers under steady state conditions, this simplification is equivalent to assuming that the decay of a contaminant through surface and groundwater pathways is the same. This assumption deserves more discussion and is simply given for granted in the current model description.

Then, taking into account the above assumptions, the runoff rate K_Q (m d^{-1}) is simply:

$$K_Q = 0.001 \cdot \frac{Q\ \cdot R_{liq}}{\theta} / 365$$

where Q is the annual discharge per unit area (mm y^{-1}).

Degradation

The degradation processes in the soil compartment are specified by the degradation rate $K_{deg,s}$ (s^{-1}) as follows:

$$K_{\deg,s} = \alpha_s \exp(\beta_s T)$$

where α_s (s^{-1}) and β_s (K^{-1}) are the degradation coefficients and top soil temperature *T (K)* is assumed to be equal to the atmospheric one.

Total soil removal rate

The overall removal rate in soil K_{soil} (d^{-1}) is

$$K_{soil} = \frac{86400 \cdot (K_{er} + K_{vl}) + K_Q}{h} + 86400 \cdot K_{\deg,s}$$

where *h* (m) is the soil layer thickness, set to 0.3m.

Water loads

The rate of chemical load in liquid form to surface water bodies, $Load_Q$ (d^{-1}), computed as a fraction of the emission to soils in each cell (emission being direct emission to soil, or deposition from the atmosphere, or the sum of the two), is given by:

$$Load_Q = \frac{K_Q}{h}.$$

Sediment loads

Similarly, the rate of chemical sediment load to surface water bodies, $Load_S$ (d^{-1}), computed as a fraction of the emission to soils in each cell (emission being direct emission to soil, or deposition from the atmosphere, or the sum of the two), is given by:

$$Load_S = \frac{86400 K_{er}}{h}.$$

The soil compartment of MAPPE Global, oppositely to the atmospheric one, is considered as sufficiently matured and presently no further development of this part of the model is planned.

2.3 Ocean compartment

Water-suspended solids partitioning

In the sea environment, the chemical partitioning between solid and liquid phase is calculated on the basis of the particulate organic carbon POC (kg l^{-1}) suspended in sea water. The POC is estimated according to Legendre and Michaud (1999), as:

$$POC = 10^{-6.79} \chi^{0.51}$$

where χ being the concentration of chlorophyll (µg L^{-1})[1].

Then, the mass fraction of chemical in particulate phase Φ' (-) is:

$$\phi' = \frac{0.41 K_{ow} POC}{1 + 0.41 K_{ow} POC}$$

[1] Legendre and Michaud (1999) propose the equation log(POC)=2.21+ 0.51 log χ, with both POC and χ in mg m^{-3}. The term $10^{-6.79}$ arises from converting POC into kg l^{-1}.

Volatilization

The velocity of volatilization from the sea surface to air, $K_{sea,\ vol}$ (m s^{-1}), is evaluated consistently with the two-resistance model for gas absorption, and is:

$$K_{sea,vol} = K_{gas,water} K_{aw} (1 - \phi')$$

Sinking with organic carbon

The velocity of sinking with organic particles, $K_{sea,\ settl}$ (m s^{-1}), is:

$$K_{sea,settl} = \phi' \frac{F'_{OC}}{86400 * POC}$$

where F'_{OC} is the sinking flux of *POC*. The F'_{OC} (Mg m^{-2} day^{-1}) is evaluated according to Baines et al. 1994 (see also Dachs et al., 2002)[2] as:

$$F'_{OC} = 10^{-6.91} \chi^{0.81}$$

Degradation

The degradation processes in the ocean compartment are specified by the degradation rate $K_{deg,w}$ (s^{-1}) as follows:

$$K_{\deg,w} = \alpha_w \exp(\beta_w T)$$

where α_w (s^{-1}) and β_w (K^{-1}) are the degradation coefficients and the water temperature *T* is in Kelvin degrees.

Total ocean removal rate

The total ocean removal rate K_{sea} (d^{-1}) is:

$$K_{sea} = 3600 \cdot \left(\frac{K_{sea,settl} + K_{sea,vol}}{MLD} + K_{\deg,w} + \frac{u}{X} \right) \cdot 24$$

where *MLD* (m) is the ocean mixing layer depth, *u* (m s^{-1}) is the average ocean current velocity and *X* (m) is the size of the calculation cells (approximately *100000* m corresponding to 1 degree spatial resolution).

Similarly to the air compartment, in the expression for total oceanic removal rate the term *u/X* accounts for intramedium advection transfer, and should be considered for an isolated emission which is an ideal extreme case.

The other extreme case is when emissions occur in a uniform way in space, and advection may be neglected. In this case, one should consider K'_{sea} (d^{-1}) no advection:

$$K'_{sea} = 3600 \cdot \left(\frac{K_{sea,settl} + K_{sea,vol}}{MLD} + K_{\deg,w} \right) \cdot 24$$

Again, the real situations should lie in between these extremes.

No further development of the oceanic compartment of MAPPE Global is foreseen at this stage but obviously the eventual incorporation of the directions of the ocean currents will improve the simulation of the contaminant fate in oceans and seas.

[2] Baines et al., 1994, propose the equation $\log(F'_{OC}) = 2.09 + 0.81 \log \chi$, with F'_{OC} in mg m^{-2} day^{-1} and χ in mg m-3. The term $10^{-6.91}$ arises from converting F'_{OC} into Mg m^{-2} day^{-1} to be divided by POC in kg l^{-1} or Mg m^{-3}.

2.4 Inland water compartment

The inland water compartment is only accounted for as a "transitional" one, through which loads from soil are transferred to oceans, passing through an exponential decay process accounting for the inland retention time of the fresh water. The single parameter that accounts for possible retention is the average retention time of catchments τ (d).

Thus, the rate of load to oceans (d^{-1}) through the surface water, as a fraction of emissions (direct or indirect) occurring in soil, is given by:

$$Load = \frac{1}{A}\int_A \left(Load_Q e^{-\frac{\ln(2)\tau}{dt_{50,w}}} + Load_S e^{-\alpha\frac{\ln(2)\tau}{dt_{50,s}}} \right) dA$$

where A is the catchment area, $dt_{50,\,w}$ (d) and $dt_{50,\,s}$ (d) are the half-lives of the chemical in dissolved and sediment phase, respectively, while α is the ratio of the residence time of sediments and the residence time of water in the catchment (see Pistocchi, 2008).

At the present stage of development of the MAPPE Global model, due to the practical difficulty to assign a value of α for each catchment, and considering the uncertainty in half lives in sediments and in *SSY*, we simply assume that all load with sediments is eventually delivered to the oceans, i.e. α=0 meaning that the exponent in the second term in the above integral is just unit. Moreover, assuming that τ is a single value for each catchment and the half-life is a non-spatially variable but chemical specific constant, the above expression simplifies to:

$$Load = \frac{1}{A}\left(\int_A Load_Q dA \right) e^{-\frac{\ln(2)\tau}{dt_{50,w}}} + \frac{1}{A}\left(\int_A Load_S dA \right)$$

In practical terms, the expressions $\left(\int_A Load_S dA \right)$ and $\left(\int_A Load_Q dA \right)$ are computed in GIS as "zonal operators" with statistics "average" on zones given by the catchments considered in the MAPPE Global model.

In the moment no further development of the inland water compartment of the MAPPE Global is foreseen.

3. Data used for model parameterization

The data used in the equations described in the previous chapter are summarized in **Error! Reference source not found.**, where we distinguish three types of parameters:

- parameters representing measurable, physico-chemical properties of a specific substance (type I);
- parameters representing environmental variables known or assumed to directly influence fate (type II);
- parameters used as proxies or input to compute environmental variables known or assumed to directly influence fate (type III).

Whenever parameters are in the form of a geographic dataset (map), detailed documentation can be found in Zulian et al. (2010).

Parameter	***Meaning***	***Estimate***	***Type***
X	Grid cell size	Spatial resolution of 1^o (ca.100km)	III
MW	Molecular weight	Chemical specific	I
K_{deg}	Compartment specific degradation rate	Chemical specific	I
α, β	Compartment specific degradation coefficients	Chemical specific	I
T	Compartment specific temperature (K)	Global Map	II
ABL	Atmospheric boundary layer height	Global map	II
K_{aw}	Air-water partitioning coefficient	Chemical specific	I
K_{aw0}	Air-water partitioning coefficient at reference temperature	Chemical specific	I
P	Annual average precipitation rate	Global map	II
γ	Temperature dependence coefficient for Kaw	Chemical specific	I
K_{ow}	Octanol-water partitioning coefficient	Chemical specific	I
K_{oa}	Chemical octanol-air partition coefficient	Chemical specific	I
OC	Concentration of particulate organic carbon in the atmosphere	Global map	II
S	Scavenging factor	Default value: $2 * 10^5$	III
F_{OC}	Deposition flux of atmospheric particulate organic carbon	Global map	II
$V_{f,d}$	Absorption velocity of atmospheric chemicals in gas phase for deciduous forests	Default value: 0.036 m s^{-1}	III
$V_{f,b}$	Absorption velocity of atmospheric chemicals in gas phase for evergreen broadleaved forests	Default value: 0.072 m s^{-1}	III
$V_{f,c}$	Absorption velocity of atmospheric chemicals in gas phase for evergreen conifer forests	Default value: 0.0078 m s^{-1}	III
Dec	Percentage of deciduous forest cover (% of the grid cell)	Global map	III
Eve	Percentage of evergreen forest cover (% of the grid cell)	Global map	III
Bro	Percentage of broadleaved forest cover (% of the grid cell)	Global map	III
h_s	Half of the soil layer thickness	Default value: 15 cm	III
ξ	Tortuosity factor	Default value: 13.6	III
θ	Soil porosity – Common to the soil compartment	Default value: 0.4	III
ω	Soil water content – Common to the soil compartment	Default value: 0.2	III

Parameter	*Meaning*	*Estimate*	*Type*
d_a	Thickness of the laminar micro layer at the air-soil interface	Negligible comparing to h_s ξ	III
D_a	Diffusion coefficient of the chemical in air on soil	Chemical specific	III
u_{10}	Wind speed at 10 m height in air	Global map	II
Imp	Impervious surface cover: % of the grid cell	Global map	II
w	Water cover: % of the grid cell	Global map	II
ρ	Soil bulk density	Default value: 1.4	II
K_d	Chemical solid-liquid distribution coefficient	Global Map	I
OCs	Organic carbon content of soils	Global map	II
SSY	Specific sediment yield	Global map	III
Q	Runoff discharge per unit area to the stream network	Global map	II
h	Soil layer thickness	Default value: 0.3 m	III
POC	Particulate organic carbon suspended in sea water	Modeled on the chlorophyll concentration map	III
χ	Chlorophyll concentration	Global map	III
F'_{OC}	Sinking flux of POC	Model (Baines et al., 1994)	II
MLD	Ocean mixed layer depth	Global map	II
u	Average Ocean current velocity	Global map	II
τ(d)	Average retention time of catchments	Global map	II
A	Catchment Area	Global map	II
$DT_{50,w}$	Half live of the chemical in dissolved phase	Chemical specific	I

Table 1 – parameters used in the model (the "types" are explained in the main text). The list of the model parameters is structured following the categories: general, atmospheric, soil, ocean and surface water (all given in different colors).

4. Model verification

In order to evaluate the performance of the MAPPE Global model a comparison with established Life Cycle Impact Assessment models, such as Impact World (Shaked et al., 2008) and USEtox (Rosenbaum et al., 2008), was made. Keeping in mind the limitations of MAPPE Global as well as specific features of the other models (e.g. accounting of advection, spatial resolution, etc.) the comparison covered only crosschecking of the intermedia removal rate coefficients.

Additionally, the impact of the ambient temperature on the removal rates is also studied.

4.1 Comparison of intermedia transfer rates

The analyses have been done by means of a multimedia substance as γ-hexachlorocyclohexane (Lindane) – a pesticide still used in Asia but forbidden in EU countries – which, due to its physico-chemical properties, relatively higher solubility and lower polarity (see details in Table 2), could be found in all environmental compartments. The motivation to choose Lindane is based on the assumption that, for multi-partitioning chemicals, it is expected that both the removal rates and fate vary more according to environmental parameters than for the single media chemicals (e.g. flyers, hydrophilic, etc.).

MW	Kow	Kaw	Kh	air decay rate	soil decay rate	water decay rate
[g/mol]	[-]	[-]	$Pa.m^3.mol^{-1}$	[1/s]	[1/s]	[1/s]
291	5.01E+03	2.08E-04	5.14E-01	1.85E-07	1.13E-08	1.13E-08

Table 2 - physico-chemical properties of γ-hexachlorocyclohexane (Lindane).

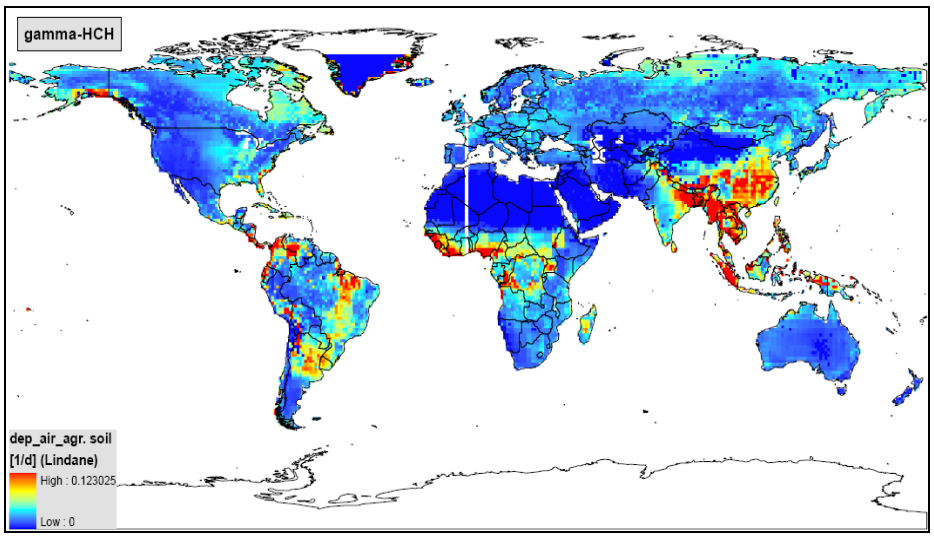

(a) – over agricultural or natural soil

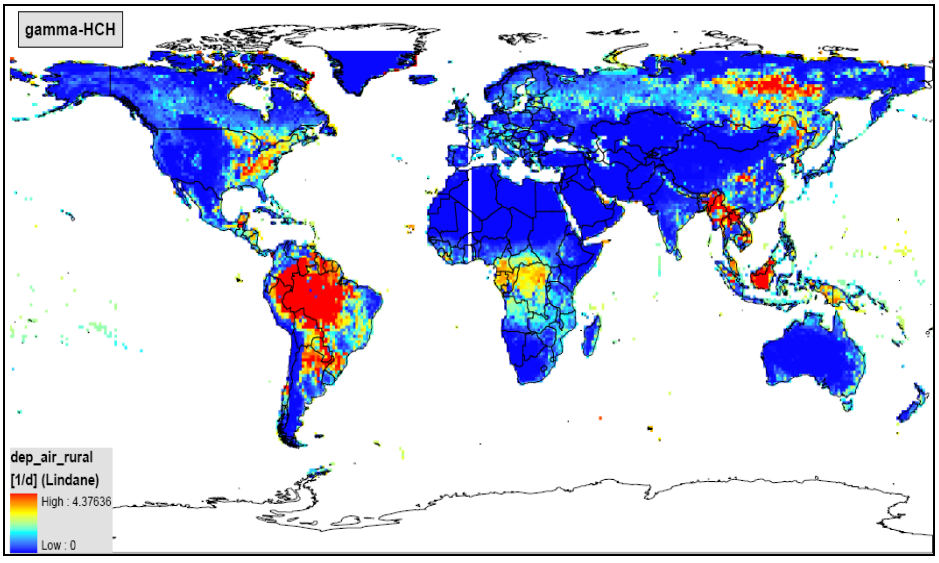

(b) – over rural and forested areas

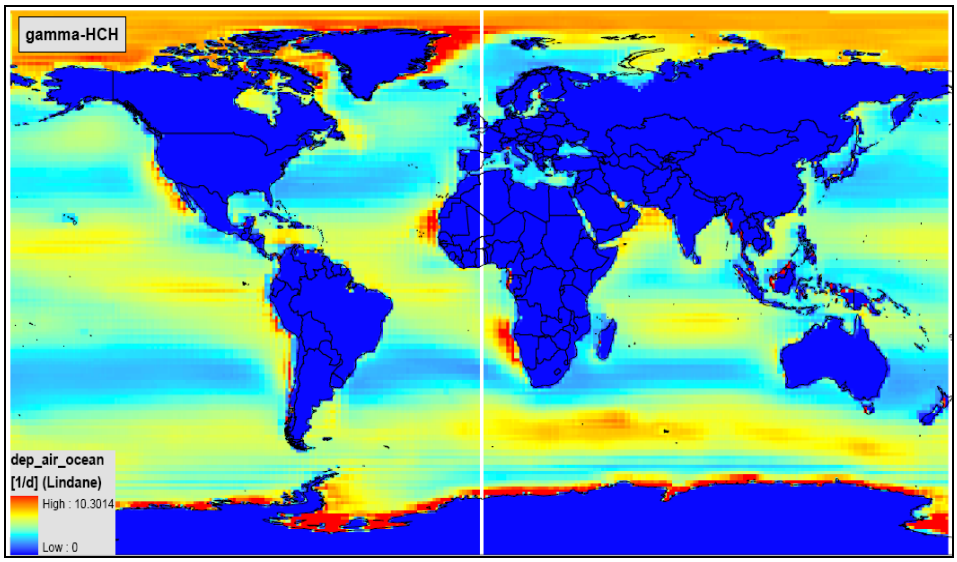

(c) – over oceans and seas

Figure 2 - MAPPE global map of atmospheric deposition rate (d^{-1}) for Lindane.

For instance, examples of MAPPE Global transfer out of the cells for the atmospheric compartment, quantified by the air deposition rate (sum of wet and dry deposition plus gas exchange; see also the formulas in chapter 2.1) over the agricultural/natural and rural/forest areas and above the ocean surface, assuming unit atmospheric emission everywhere on the Globe, are presented in Figure 2.

Furthermore, respecting the different spatial resolution of the considered models, the results of MAPPE Global were aggregated per continents (considering also the important Asian industrial states like China, India and Japan), per oceans and European seas, or according to the typical zonation used in Impact World model. Then, the collective MAPPE Global results were compared with the rates produced by Impact World according its original delimitation zones and also with the "continental" average estimates of USEtox model.

Firstly, results for the atmospheric transport rates to soil, found by the three models, were contrasted as presented on Figure 3. In fact, Impact World considers only agricultural soil while USEtox employees also the rural soil type but the values for both categories actually were equal. The forecasts of MAPPE Global for zones with agricultural/natural land cover were on average 6.4 (2.76-12.68) times lower than Impact World and 4.3 (1.91-8.60) times lower than USEtox. Oppositely, it was found that the MAPPE results about air deposition over rural and forested areas are 10 times higher comparing to what the other two models calculated for soil (see Figure 3). A possible reason for these deviations could be the different way of calculation of chemical gas exchange between air and cultivated or forested land. For instance, in MAPPE Global the gas exchange from cultivated soil is missing the additional impact of plants while their effect is very well seen in the case of rural and forested areas leading to one order of magnitude higher atmospheric deposition.

In similar way, the intermedia transfer from air to fresh water and oceans/seas was compared. For the surface water, on average MAPPE Global underestimates 7.7 times the air transfer coefficients comparing to Impact World (coefficients range between 1.1 - 37.99 [y^{-1}], mean= 2.31 [y^{-1}]; however 39% overestimation for Europe, North and South America was observed) and 5.9 times underestimates USEtox transfer rates (2.956[y^{-1}]; but an overestimation by 41% for North and South America was registered). Oppositely, for the air-ocean transfer MAPPE overestimates 2.2 times Impact World (range 67.95 – 295.8, mean=90.24 [y^{-1}]) and 15 times USEtox (10.78 [y^{-1}]).

Based on the previous MAPPE Global results about the air intermedia transfer coefficients of Lindane to agricultural soil and surface water aggregated per continents plus the biggest Asian industrial states (China, India and Japan) and to marine environment, we tried to find the correspondence with estimates produced by Impact World and USEtox (see Figure 4). In general, MAPPE Global underestimates the air transfer to the other environmental compartments, apart from the convey to oceans/seas, which is actually overrated. The overall correlation, when the three models are compared, is R^2=0.31, but it significantly rises to R^2=0.85, when only MAPPE Global and Impact World models were evaluated.

The same approach has been used to evaluate the MAPPE Global results related to the removal rates from the other media. Thus, the estimates of MAPPE Global for the exchange between ocean and atmosphere are 2 and 5 times higher in comparison with results of USEtox and Impact World, respectively.

At the end, a correlation of R^2=0.18 between MAPPE Global and Impact World is found when comparing the transfer from soil to fresh water (MAPPE undervalued Impact World), while the USEtox forecast is about 9-10 times less in contrast to MAPPE Global. Oppositely, MAPPE Global underestimates the export from soil to atmosphere by one order of magnitude in distinction to USEtox and by 2 orders comparatively to Impact World.

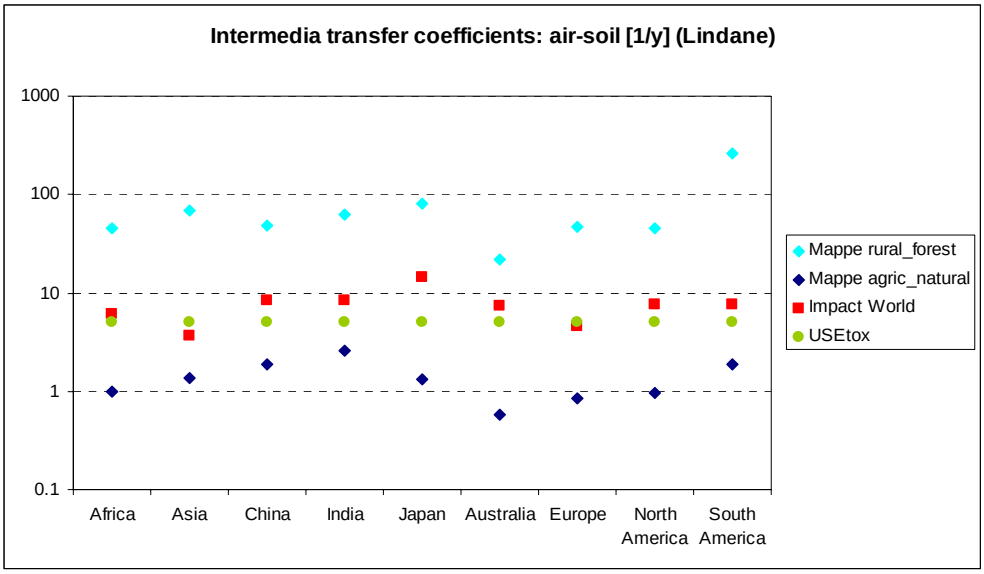

Figure 3 – comparison of MAPPE Global results about air transfer of Lindane to rural-forested and agricultural-natural soil aggregated per continent and the important Asian industrial states (China, India and Japan) with estimates of Impact World (mean= 7.76 [y^{-1}], range 1.62 - 14.62) according its original delimitation and USEtox results (4.99 [y^{-1}]) .

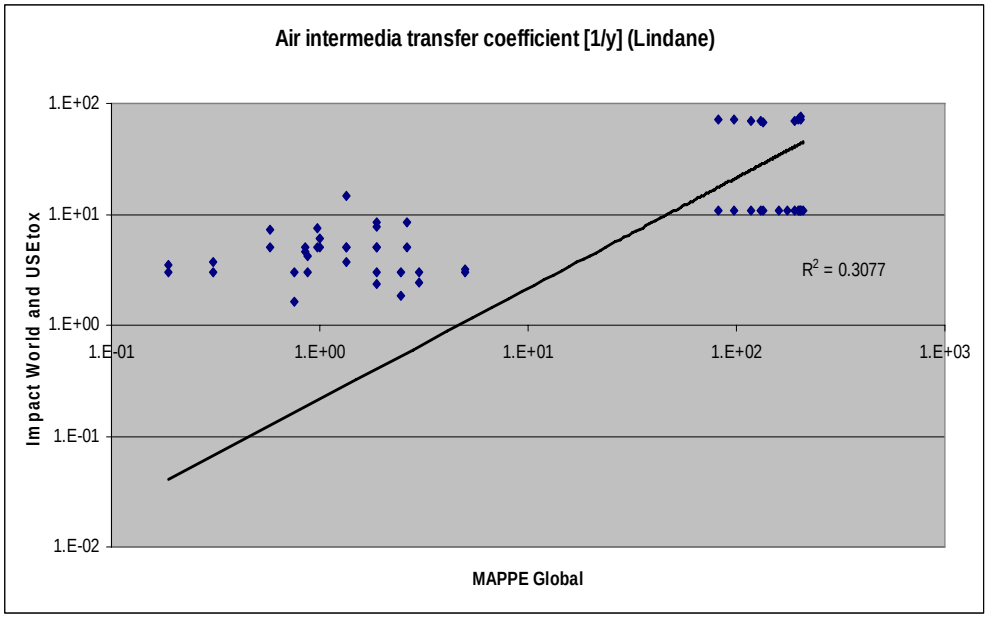

Figure 4- Correlation of air intermedia transfer coefficients (advection excluded) for Lindane to agricultural soil and surface water aggregated per continent plus the biggest Asian industrial states (China, India and Japan) and to seas/oceans calculated by MAPPE Global versus estimates produced by Impact World and USEtox (the correlation raises to R^2=0.85, if only MAPPE and Impact World are compared).

4.2 Effect of ambient temperature on removal rates

It's worth to stress again that, potentially, one additional source for the changeability of the intermedia transfer rates is related to the influence of temperature on the spatial variability of the substance physical chemical properties. To assess this influence, MAPPE Global was run considering the impact of variation with temperature of Kaw (see an example for Lindane on Figure 5a; up to 3 orders of magnitude of Kaw variability could be seen) and Kdeg (for Lindane the variability is one order of magnitude) on the total removal rates (excluding advection) against the case of application of a single global mean value for these parameters, as usual practice in fate modelling (USEtox or Impact World among the others).

However, the comparison for Lindane demonstrated that for multimedia chemicals the impact of ambient temperature seems to be low as shown in the Figure 5b, because the medians and the range of variability of results with and without accounting environmental temperature are quite similar.

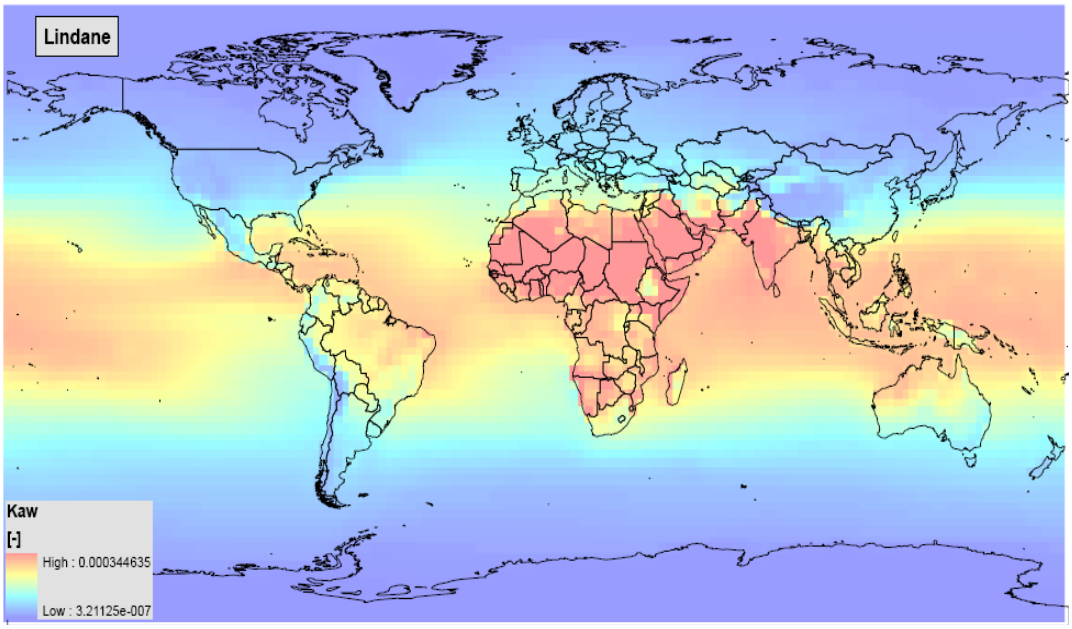

(a) – spatial variability of air-water partition coefficient Kaw (mean=$6.8*10^{-5}$; std. dev.=$6.8*10^{-5}$)

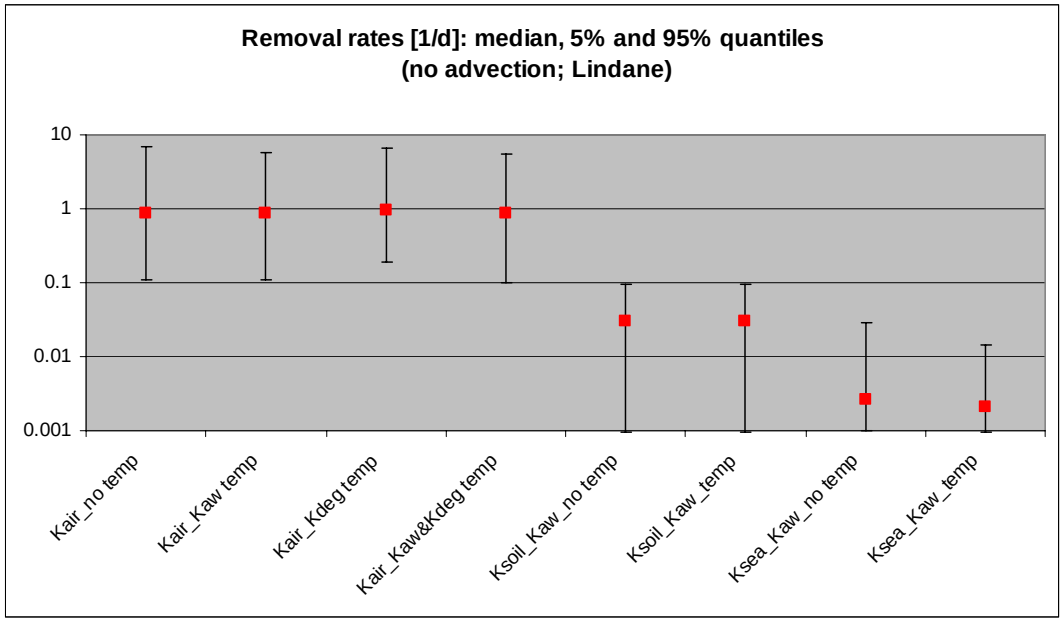

(b) – medians and range of variability (given by 5 and 95 quantiles) of air removal rate accounting no impact or dependence from temperature of air-water partitioning Kaw or degradation rate Kdeg coefficients

Figure 5 - Effect of ambient temperature on total removal rates (no advection case) for Lindane according to MAPPE Global model.

5. Analysis of spatial variability of removal rates

5.1 Representative test set of 34 chemicals

Aiming to study the spatial differentiation of environmental fate of chemicals or to perform comparison between different models a "test set" of 34 organic substances is adopted. The names of the test chemicals and their physical chemical properties used to run the MAPPE model are listed in the Table 3.

The test set comprises compounds having a large diversity of physical chemical properties in order to be representative, as far as possible, and also to reveal the potential differences in their environmental behaviour. In addition the set of considered substances is structured in 14 classes (1a, 2a, 2b, etc.) referring to specific combinations of Kow and Kaw in the chemical space.

Chemicals	Class	CAS	MW [g/mol]	Kow [-]	Kaw [-]	Air decay rate [1/s]	Soil decay rate [1/s]	Water decay rate [1/s]
Tetrachloroethylene	1a	127-18-4	166	7.59E+02	7.15E-01	3.50E-07	1.13E-07	1.10E-07
Carbon tetrachloride	1a	56-23-5	154	4.37E+02	1.11E+00	1.13E-08	3.19E-08	1.13E-07
Butadiene	1a	106-99-0	54	9.77E+01	2.97E+00	1.13E-08	3.50E-07	1.13E-07
Methomyl	2a	16752-77-5	162	3.98E+00	7.43E-09	3.32E-06	3.83E-07	3.49E-08
Acephate	2a	30560-19-1	183	1.41E-01	2.02E-11	5.59E-06	3.64E-06	1.50E-07
Formaldehyde	2b	50-00-0	30	2.24E+00	1.36E-05	5.31E-05	3.50E-06	2.01E-06
PCBs	3a	1336-36-3	292	1.26E+07	1.68E-02	4.07E-07	2.14E-07	5.70E-07
Phthalate, di(n-octyl)	3a	117-84-0	391	1.26E+08	1.04E-04	1.03E-05	5.72E-07	5.73E-07
Benzene, hexabromo-	3a	87-82-1	551	1.17E+06	1.13E-03	5.73E-09	1.34E-07	1.34E-07
Cypermethrin	3a	52315-07-8	416	3.98E+06	7.75E-06	1.07E-05	1.54E-07	1.60E-06
Mirex	3b	2385-85-5	546	7.94E+06	3.27E-02	1.13E-06	3.50E-09	1.13E-06
Trifluralin	3b	1582-09-8	336	2.19E+05	4.16E-03	1.13E-06	1.13E-07	1.13E-07
Dicofol	3b	115-32-2	370	1.05E+05	9.77E-06	1.72E-06	1.32E-07	2.14E-07
p-Dichlorobenzene	4a	106-46-7	147	2.51E+03	9.73E-02	3.50E-07	3.50E-08	1.13E-07
Aldrin	4a	309-00-2	365	1.02E+03	1.78E-03	3.86E-05	1.13E-08	1.10E-08
1,1,2,2-Tetrachloroethane	4a	79-34-5	168	2.45E+02	1.48E-02	1.13E-08	3.50E-08	1.13E-07
Captan	4a	133-06-2	301	2.00E+02	2.62E-07	1.13E-05	3.50E-07	1.13E-05
Pronamide	4b	23950-58-5	256	2.69E+03	3.95E-07	6.62E-06	9.97E-08	1.97E-07
Anthracene	4b	120-12-7	178	3.47E+04	2.25E-03	3.50E-06	3.50E-08	3.50E-07
gamma-HCH	4b	58-89-9	291	5.01E+03	2.08E-04	1.85E-07	1.13E-08	1.13E-08
Dimethyl phthalate	4b	131-11-3	194	1.32E+02	4.24E-06	1.13E-06	3.50E-07	1.13E-06
Methanol	5a	67-56-1	32	1.70E-01	1.84E-04	4.91E-07	3.50E-06	3.50E-06
1,2-Dichloroethane	5a	107-06-2	99	3.02E+01	4.77E-02	1.13E-07	3.50E-08	1.13E-07
Ethyl acetate	5a	141-78-6	88	5.37E+00	5.41E-03	9.92E-07	1.13E-06	2.01E-06
N-Nitrosodiethylamine	5b	55-18-5	102	3.02E+00	1.47E-04	3.21E-05	1.13E-07	3.21E-05
Thioperoxydicarbonic diamide, tetramethyl-	6a	137-26-8	240	5.37E+01	1.23E-05	1.13E-06	3.50E-07	1.13E-06

Propoxur	6b	114-26-1	209	3.16E+01	5.77E-08	3.85E-05	3.50E-07	3.50E-07
1H-Isoindole-1,3(2H)-dione, 2-(trichloromethyl)thio -	6c	133-07-3	297	7.08E+02	3.09E-06	7.87E-06	1.40E-08	1.40E-08
Benomyl	6c	17804-35-2	290	2.00E+02	1.99E-10	3.86E-05	1.13E-07	1.13E-06
Hexachlorobutadiene	7a	87-68-3	261	6.03E+04	4.16E-01	1.50E-08	1.13E-07	1.10E-07
Hexachlorocyclopentadiene	7a	77-47-4	273	1.10E+05	1.09E+00	1.97E-07	4.58E-07	2.23E-06
Heptachlor epoxide	7b	1024-57-3	389	9.55E+04	8.48E-04	2.59E-06	2.74E-08	2.74E-08
Hexachlorobenzene	7b	118-74-1	285	3.16E+05	6.86E-02	2.62E-08	3.50E-09	3.50E-09
Heptachlor	7b	76-44-8	373	1.86E+05	1.19E-02	3.50E-06	1.13E-07	3.50E-07

Table 3 - Test set of representative chemicals and their related properties. The abbreviations used stand for: MW- molecular weight, Kow - octanol-water partition coefficient, Kaw - air-water partition coefficient, Kh - Henry constant at 25°C. The set of considered substances is structured in 14 classes referring to specific combinations of Kow and Kaw in the chemical space.

The set of chemicals, used in the report, is built on the results of FP5 OMNIITOX project (http://139.191.1.195/mappe/chemical). Similar representative compounds have been used to assess multimedia fate of chemicals by Pennington et al (2005) and for model cross comparison in USEtox model (Rosenbaum et al 2008).

5.2 Variability of total removal rates

In general, the global variability of total removal rates for different chemicals and media spans from less than one up to more than four orders of magnitude depending whether or not the advection is accounted. As expected, more wide range of variability was observed for the atmosphere and least one for the soil.

Considering the atmospheric compartment, when the advection is excluded, the range of variability was 1-4 orders of magnitude, as also discussed in Sala et al.(2011), but the chemicals belonging to the same classes (e.g. groups of 3a, 4a, etc.) do not present the same range of variability as can be seen in Figure 6a. Hence, it is necessary to explore the eventual sources of variability to identify the differences in the spatial patterns.

The model results suggest that for air-no advection case, the variability of gas exchange and/or wet deposition drives the overall changeability of the *K´air*. However, when the degradation rate is low comparing to gas exchange, the variability of total air removal rates is higher and vice versa. Thus, could be concluded that for persistent chemicals the degradation, as an elimination process, regulates (eventually reducing) the range of variability of total air removal rates, which changeability is primarily associated with the wide spatial fluctuations of gas exchange or wet deposition at global scale (see also Sala et al., 2011).

The conclusion above is even more strongly valid when the advection is accounted for air (see Figure 6b). The model results indicate that the advection, for the same reasons as degradation, is the control factor reducing the total *Kair* variability up to only one order of magnitude with the exception of a few chemicals expressing higher values for gas exchange and/or wet deposition rates (e.g. 2a or 7a clusters) comparing to the degradation ones.

In addition, it was found that the variability of the total removal rates in soil (see Figure 7a) remains below 2.5 orders of magnitude but for 68% of the chemical groups (23 out of 34) the variability is not exceeding more than one order of extent.

Nonetheless, this is not the case for the ocean compartment (no advection case) since a few chemical groups like 2, 5b and 6 (see Figure 7b) in practice show no variability while for the other ones the

removal rates are highly variable (from 2 to more than 3 orders of magnitude). Moreover, it was confirmed again the role of degradation and advection (when considered) as controlling factors of the total removal rates for the soil and ocean compartments.

Besides, I i's worth mentioning that the surface water compartment shows rather homogeneous behavior for all chemical groups (see Figure 7c) with variability up to 1.5 orders of magnitude because of the specific assumptions (limitations) under which it was considered in the present version of the MAPPE Global model.

Lastly, a comparison with USEtox model was performed in order to assess the total removal rates calculated by running this multimedia model with default environmental parameters and no spatial resolution against the spatially resolved MAPPE Global model.

For instance, taking into consideration the atmosphere, as already discussed in (Sala et al., 2011), for 4 chemicals (Formaldehyde 2b, Cypermethrin 3a, Aldrin 4a and N-Nitrosodiethylamine 5a) out of 34 representative substances, the total air removal rates excluding advection, produced by both models, are almost equal. For all the tested substances, the USEtox values are below the median values calculated by MAPPE with the only exception of N- Nitrosodiethylamine. Thus for air, USEtox tends to underestimate MAPPE Global estimates between 1 and 4 orders of magnitude and the USEtox values are closer to the 5^{th} percentile of the MAPPE results for 25 out of 34 chemicals as reported in (Sala et al., 2011). For Acephate the difference is over 4 orders of magnitude, 3 orders for Carbon tetrachloride, Butadiene and Benomyl. For another 15 substances the values are within the range of one order of magnitude while for the other substances (15 out of 34 cases) the deviation is not more than 2 orders.

In summary, considering all environmental media, the comparison of total removal rates calculated by MAPPE Global and USEtox models allows to conclude that USEtox model tends to undervalue MAPPE Global estimates between 1 and 4 orders of magnitude and the USEtox values are closer to the 5th percentiles rather than to the medians of the MAPPE Global outcome.

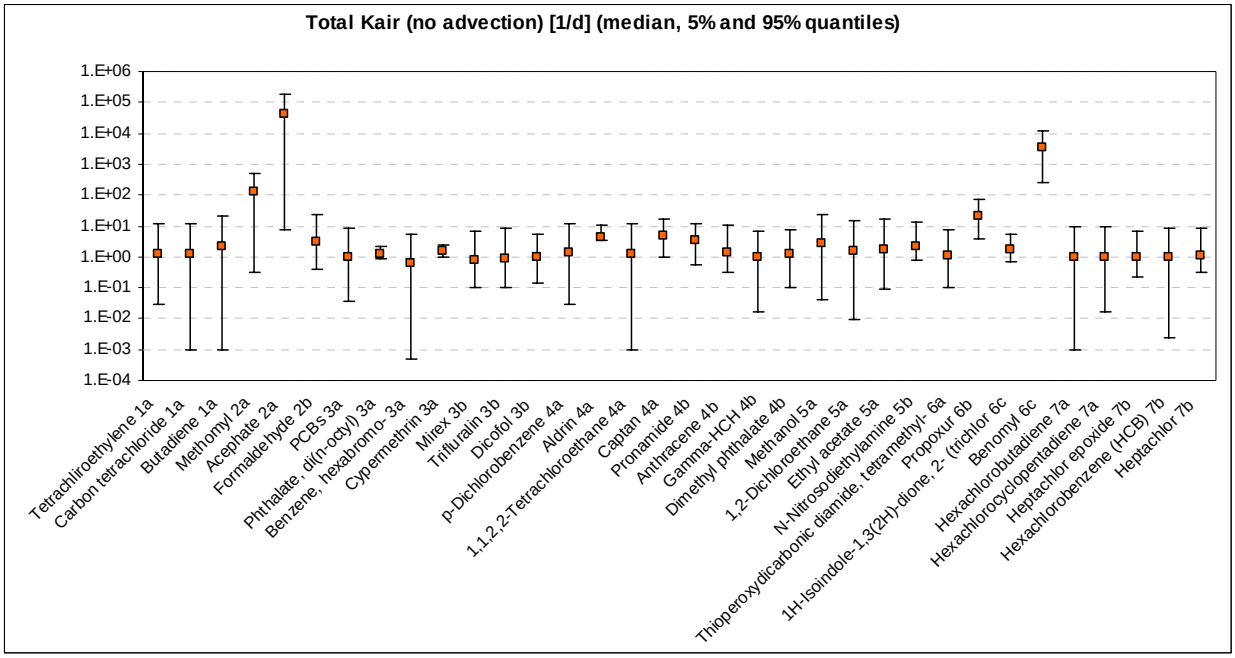

(a) – total K'_{air} no advection case

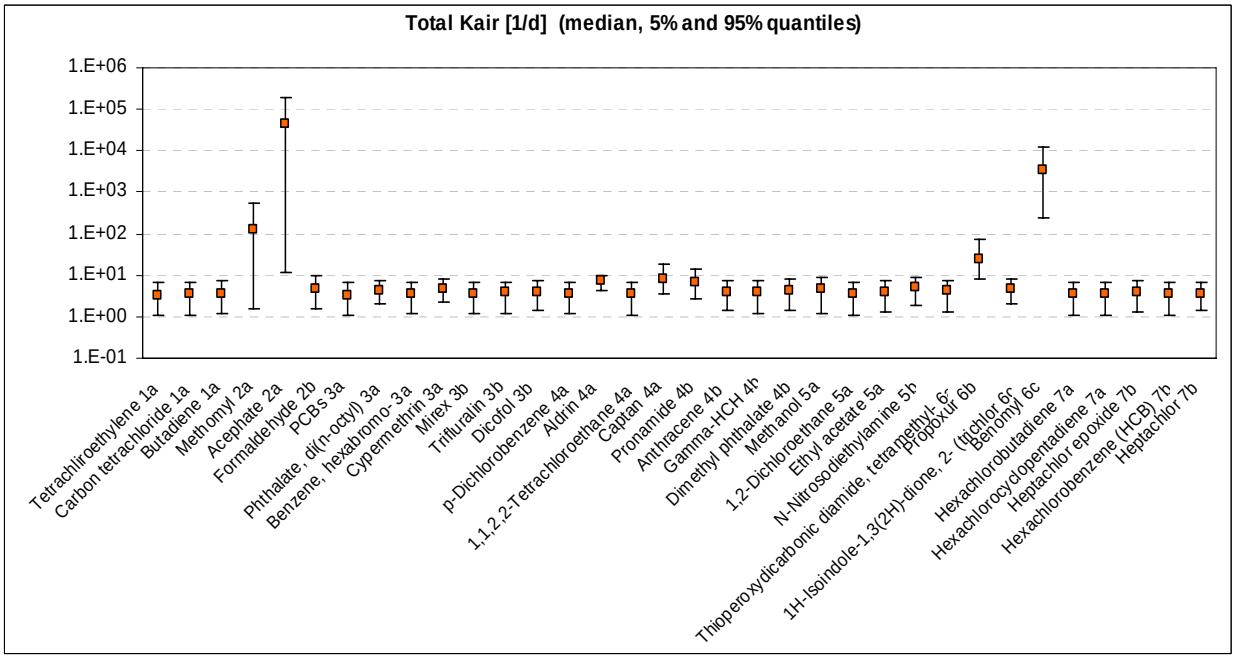

(b) – total K_{air} with advection included

Figure 6 – Global variability of atmospheric removal rates for the considered set of 34 representative chemicals.

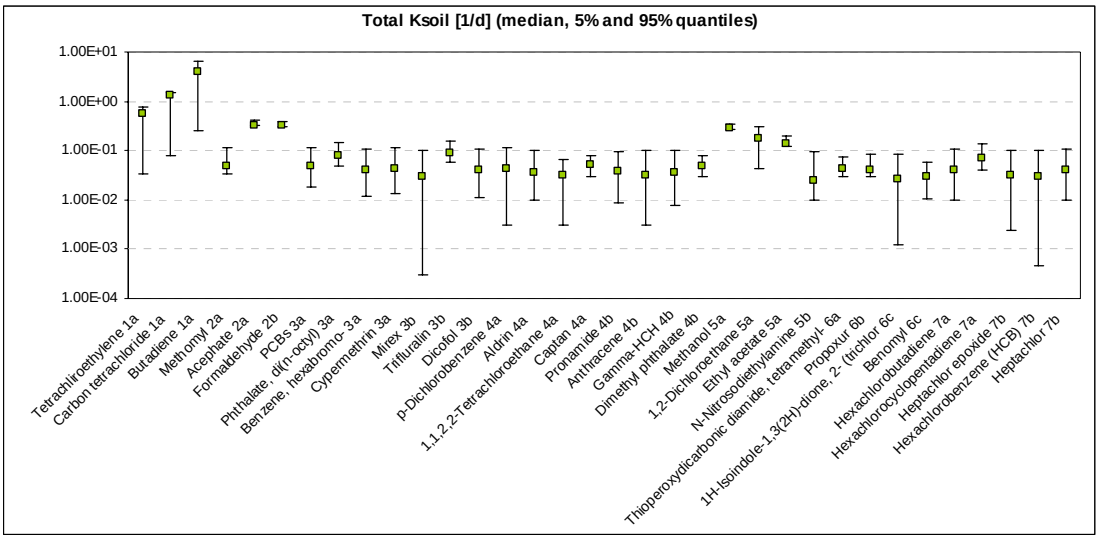

(a) – total soil removal rate K_{soil}

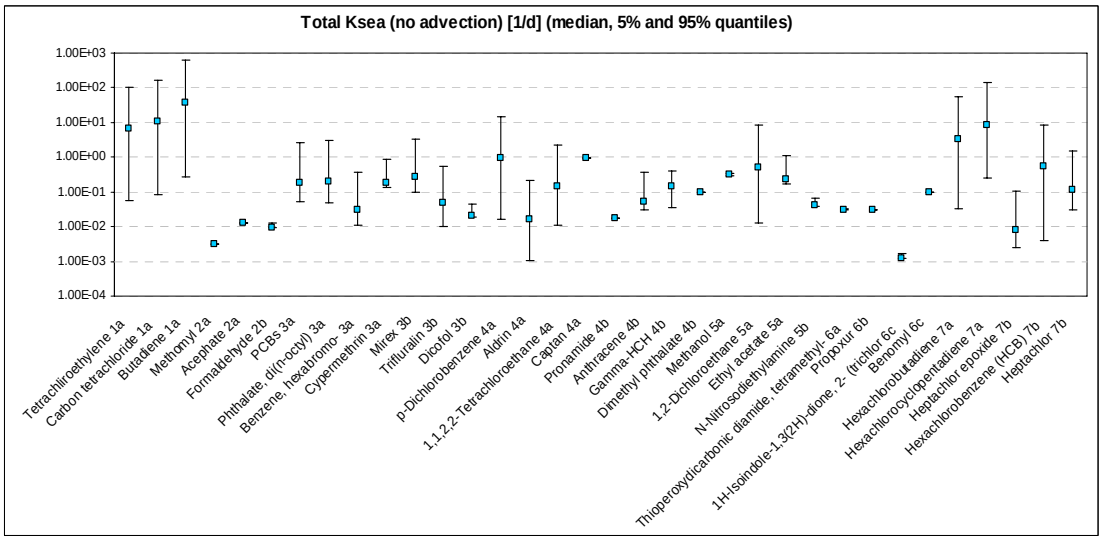

(b) – total ocean removal rate K'_{sea} (no advection case)

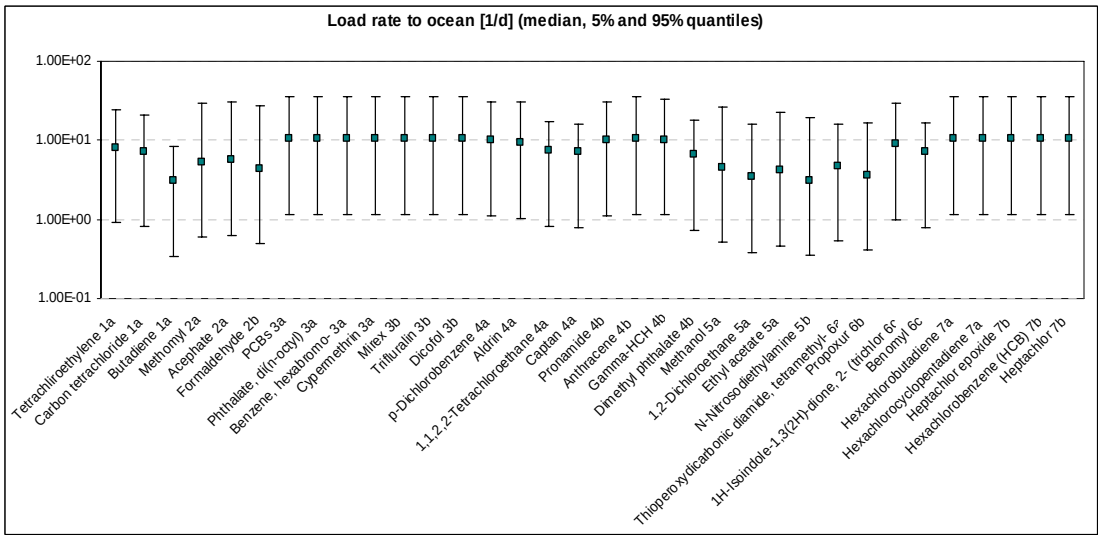

(c) - load rate to oceans through the surface water as a fraction of direct or indirect soil emissions

Figure 7 - Global variability of soil, ocean and load to ocean removal rates for the considered chemicals.

5.3 Relative importance of different removal processes

In order to identify the reason for variability and trying to answer whether or not the variability follows similar spatial patterns, distribution maps at global scale were calculated for all chemicals, listed in the Table 3. The discussion details, in particular those for the atmosphere, are provided extensively in Sala et al. (2011).

For chemicals belonging to the group 1a, the dominant fate compartment is air. Excluding again advection, it was found that the variability of the atmospheric removal rates is triggered to the gas absorption (see the example of Butadiene in Figure 8). However, for the other media the variations of chemical elimination rates of "flyers" are associated with volatilization, being in turn modulated by the gas exchange, as confirmed for Butadiene for soil (see Figure 9) and ocean (see Figure 10) compartments.

The environmental partitioning of chemicals fitting to the 2a group is related to water. According to the model results for air the higher variability of Kair-values just follows the spatial patterns of the precipitation around the Globe (keep in mind that the advection is not considered). For example, comparing the total removal rate of a highly hydrophilic chemical, such as the Acephate, with the pattern of the wet deposition (see Figure 11), it is clear that the foremost removal rate process is exactly the wet deposition.

Oppositely to atmospheric case, the removal rates of "swimmers" express low variability (up to one order of magnitude) due to the lower variations of chemical liquid fractions in soil and in ocean environment because the generally lesser Kaw reduce the volatilisation from the ocean surface (keep in mind that the advection is not considered).

For hydrophobic chemicals, such as PCBs in the 3a group, the pattern of the global variability may be explained considering air (no advection) mainly by gas absorption, in particular for forested areas. The global maps of removal rates for PCBs are not provided in the report because they are similar to those for Butadiene. However, the spatial maps for different air removal rates showed that a certain influence of particle flux could be accounted for group 3a, as the highest values in the total air removal rates (no advection) are located at the same areas where the particle dry deposition is uppermost or at zones with the elevated aerosol concentrations.

Besides, following the model results for PCBs, it was confirmed that in soil (see Figure 12) the environmental fate of the hydrophobic substances is basically regulated by the degradation (followed by erosion) while for the ocean (see Figure 13) the major removal processes were degradation and volatilisation.

In general, for the chemicals tending to partition predominantly in particulate form and depending of their persistence, we may suggest that the variability of removal rates in different media will be similar to those derived for PCBs (group 3a) but with a minor role of gas exchange and more clear effect of the particle dry deposition in air, erosion in soil and settling in ocean compartment.

Aimed at multimedia chemicals, like these in groups 4a or 4b, the pattern of global fate and the difference between total air removal rates with and without accounting advection could be followed in Figure 14 presenting results for Lindane (group 4b) as an example. Furthermore, the variability of the atmospheric removal rates of Lindane is found to be related to the interplay of different removal processes. However, the substantial contribution of the gas exchange (followed by the degradation and wet deposition) is evident since the Kgas is the prevailing removal rate compared to the others (Kpart, Kwet, and Kdeg), as presented in Figure 15 - Figure 18, respectively.

Further details about the effect of the different elimination processes in air estimated by means of a global average of the relative removal rates as a percentage from the total one is given in Table 4, again for Lindane. As can be seen, when the advection is not considered, the gas exchange accounts globally on average for 77% of the total air removal rate while the degradation – ca.18%, wet deposition – for ca.5% and particle dry deposition is quite below 1%. In the case with advection (accounting itself ca.51% of the total) the relative importance of the gas absorption and degradation is reduced to 46% (approximately by half) and 2%, respectively.

The fate of multimedia chemicals in soil is likely to be ruled by the degradation (79% of the total) and erosion (17%) while for ocean this is a combination again of degradation (75%) and volatilization (24%) according to the Lindane results provided in the Table 4. Obviously, the picture for the ocean compartment is dramatically changed whether the advection is included into consideration since it took ca.98% of the total removal rate.

Lastly, the variability of removal rates of the chemicals from the other clusters of the considered representative set, in particular these that tend to spread between two environmental media (for example water and air, etc.) or staying in a single media but appearing in different phases (for example in dissolved and particulate form in soil or in gas and aerosol phases in air) obviously will follow combinations of the patterns for the flyers, swimmers and particle-bound chemical substances.

COMPARTMENT		RELATIVE REMOVAL RATE (%)				
		Kgas	**Kwet**	**Kpart**	**Kdeg**	**Kadv**
AIR	No Advection	77.3230	4.7205	0.0002	17.9562	N.A.
	With Advection	46.4402	0.8009	0.0001	2.1495	50.6093
SOIL		**Kerosion**	**Kvol**	**Krun-off**	**Kdeg**	
		16.9001	0.6734	3.3080	79.1185	
		Ksettling	**kvol**	**kdeg**	**Kadv**	
OCEAN	No Advection	4.98E-01	23.72169	75.780235	N.A.	
	With Advection	3.99E-02	0.88736	1.01E+00	98.06723	

Table 4 – global average relative removal rates (as % from the total) for Lindane in different environmental compartments.

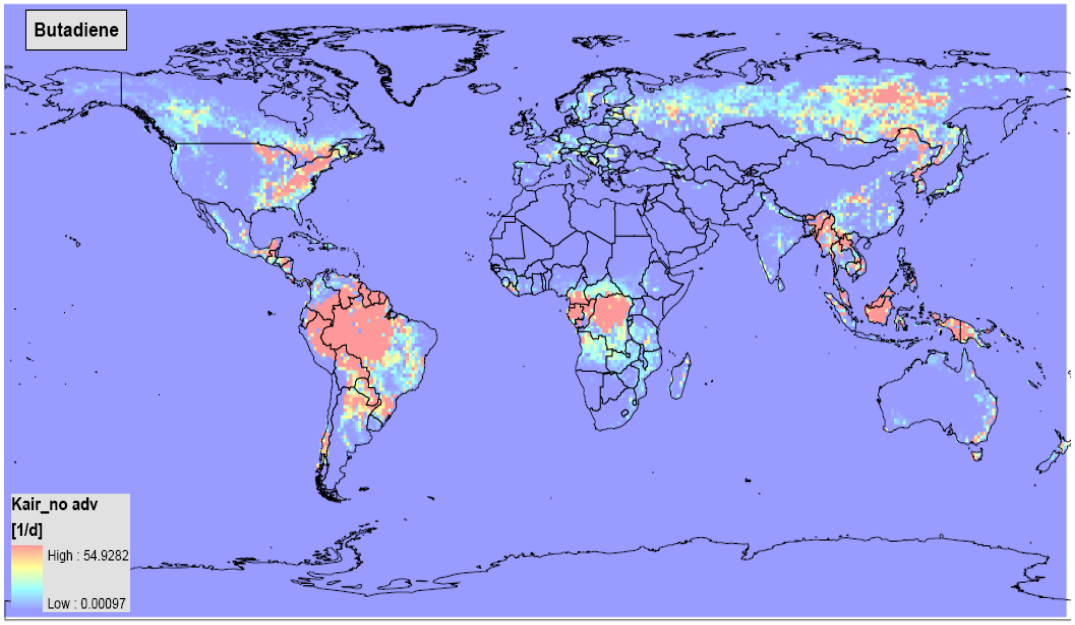

(a) – total air removal rate no advection (global mean=0.33 d^{-1}; std.dev.=2.09)

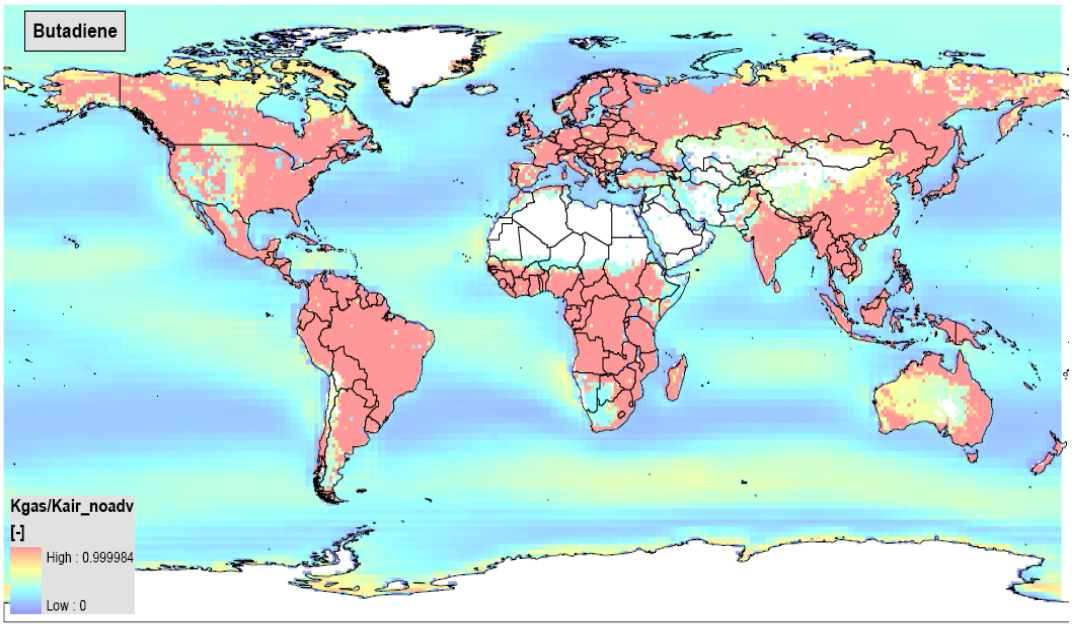

(b) –ratio of removal rate due to gas exchange to Kair_no adv (global mean=0.37; std.dev.=0.28)

Figure 8 - Maps of air removal rate of Butadiene.

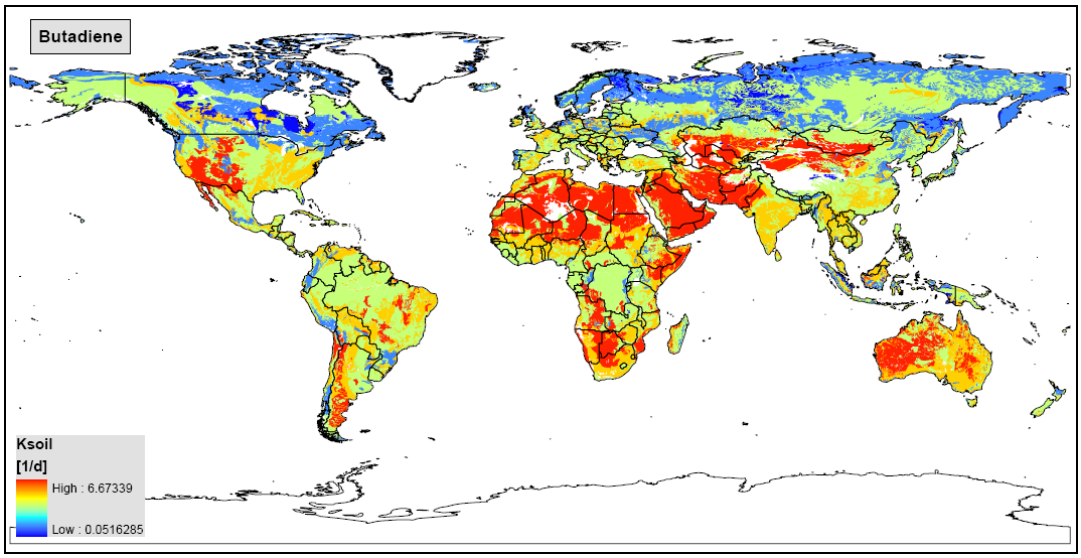

(a) – total soil removal rate (global mean=3.926 d^{-1}; std. dev.=1.744)

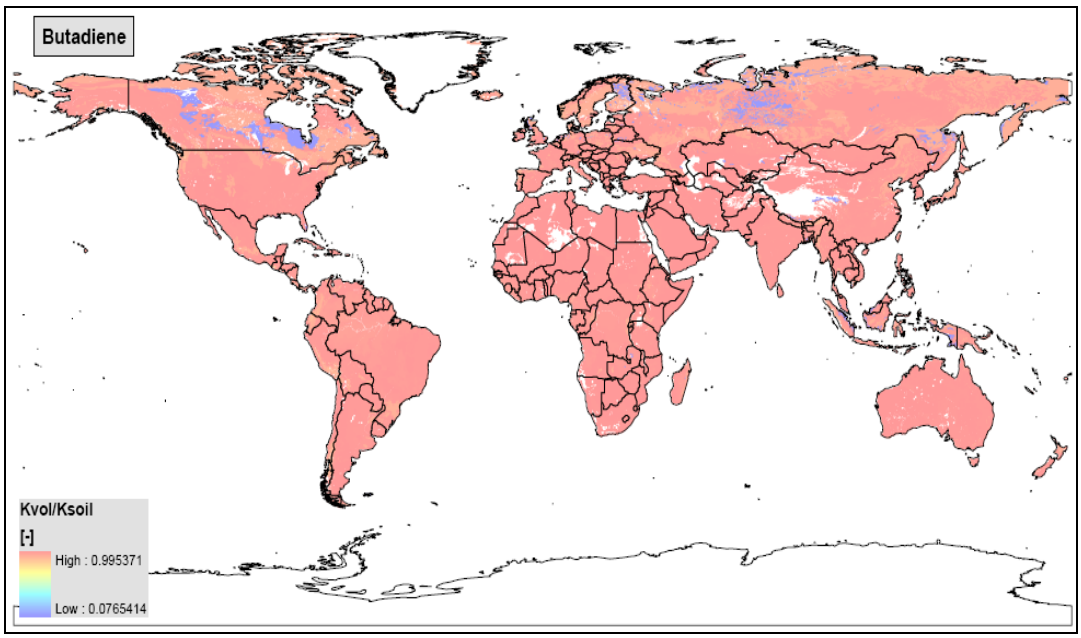

(b) – ratio of removal rate due to volatilisation to Ksoil (global mean=0.97)

Figure 9 - maps of soil removal rate of Butadiene.

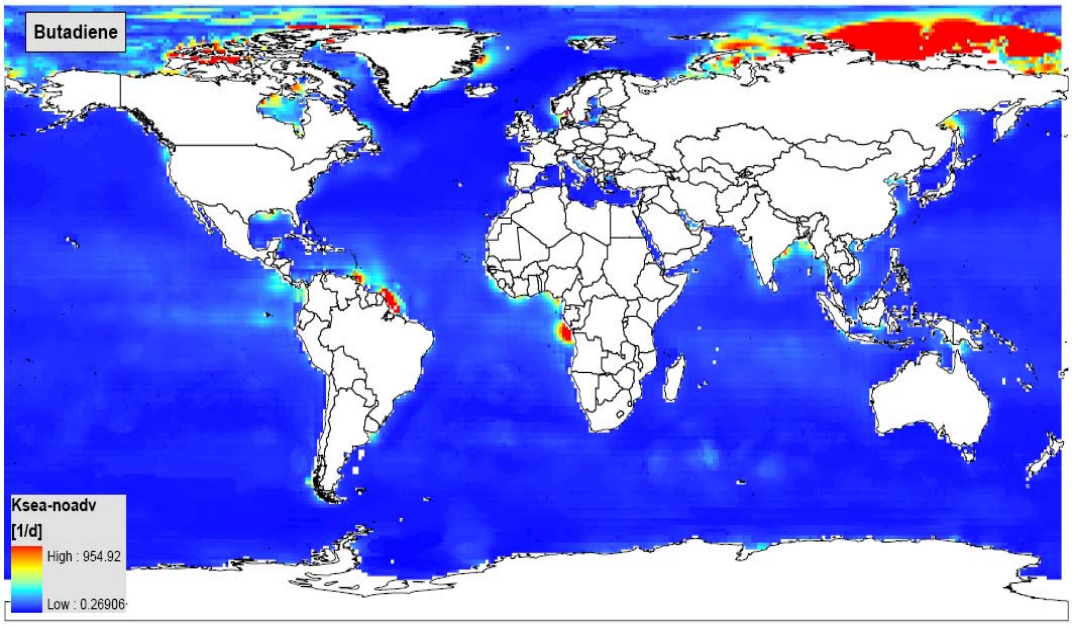

(a) – total ocean removal rate no advection (global mean=15.93 d^{-1}; std.dev.=60.14)

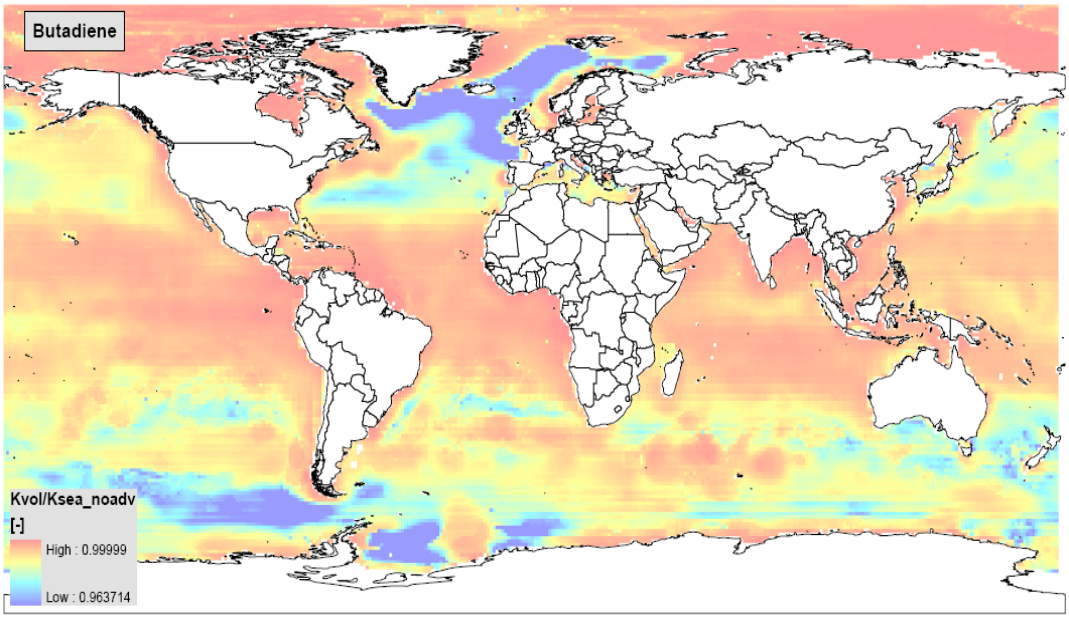

(b) – ratio of removal rate due to volatilisation to Ksea_no adv (global mean=0.99)

Figure 10 - maps of ocean removal rate of Butadiene.

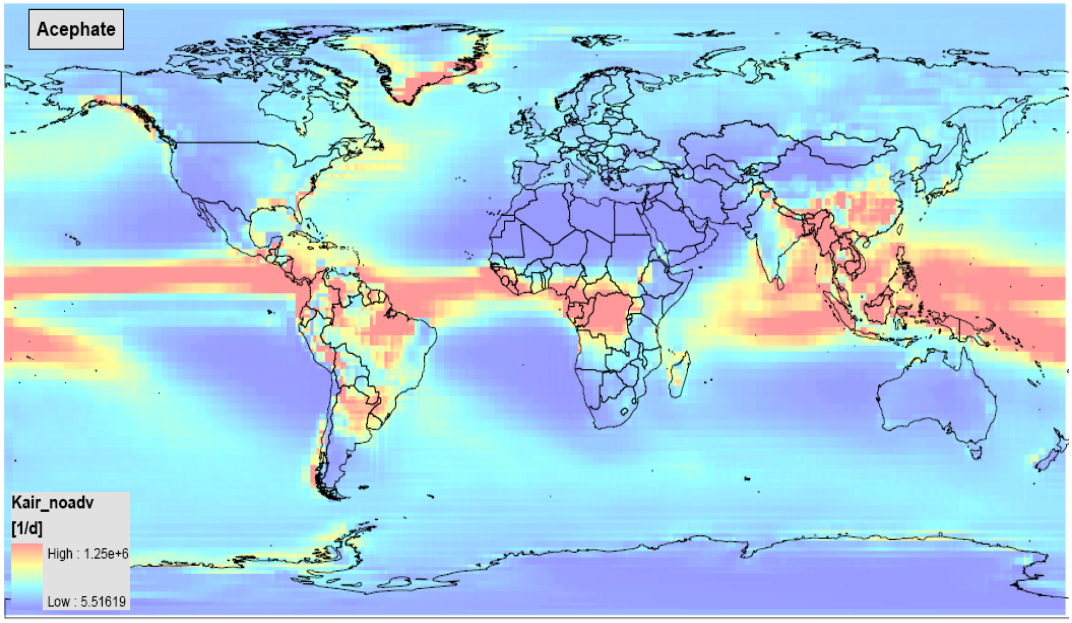

(a) – total air removal rate no advection case (global mean=45603 d^{-1}; std.dev.=47222)

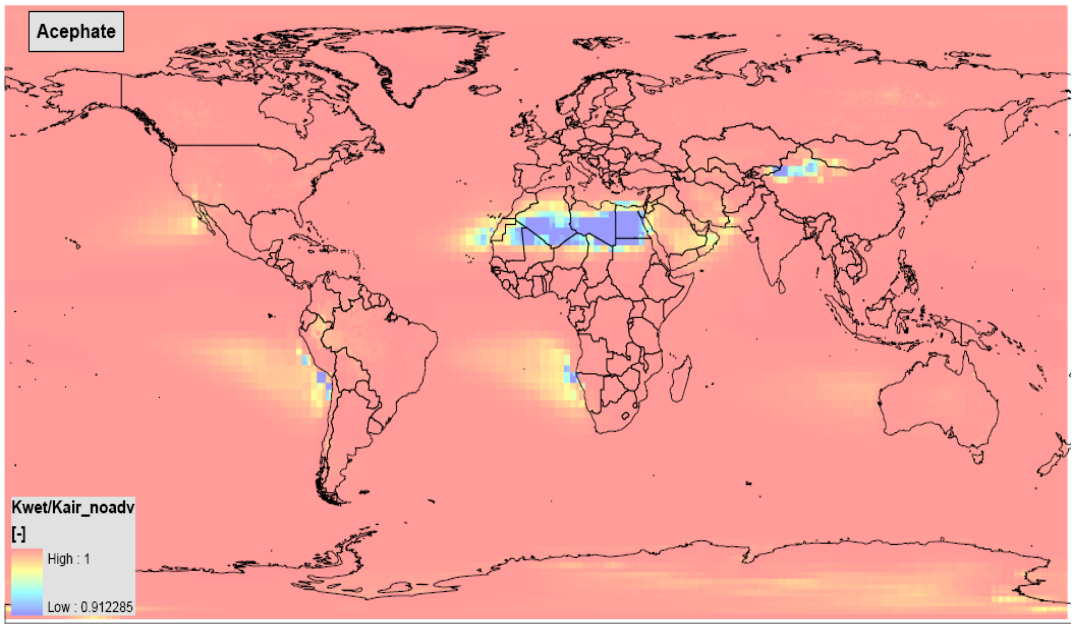

(b) – ratio of removal rate due to wet deposition to Kair_no adv (global mean=0.999)

Figure 11 - Maps of air removal rates of Acephate.

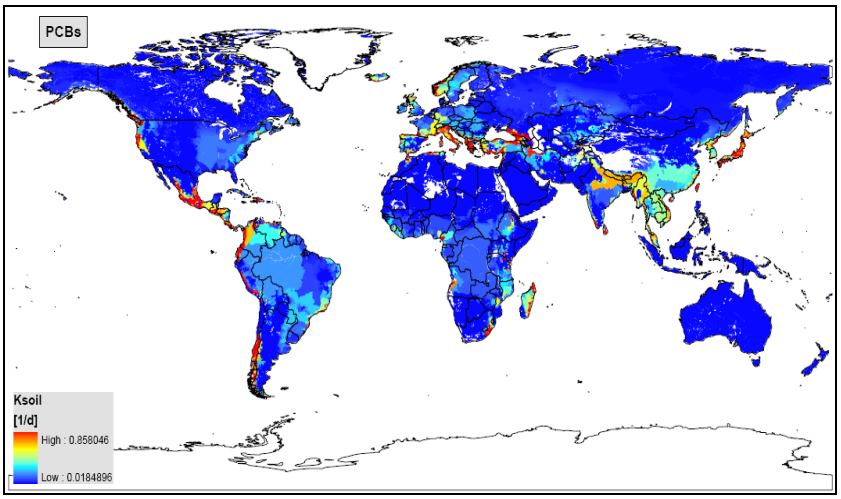

(a) - total soil removal rate (global mean=0.02 d^{-1}; std.dev.=0.002)

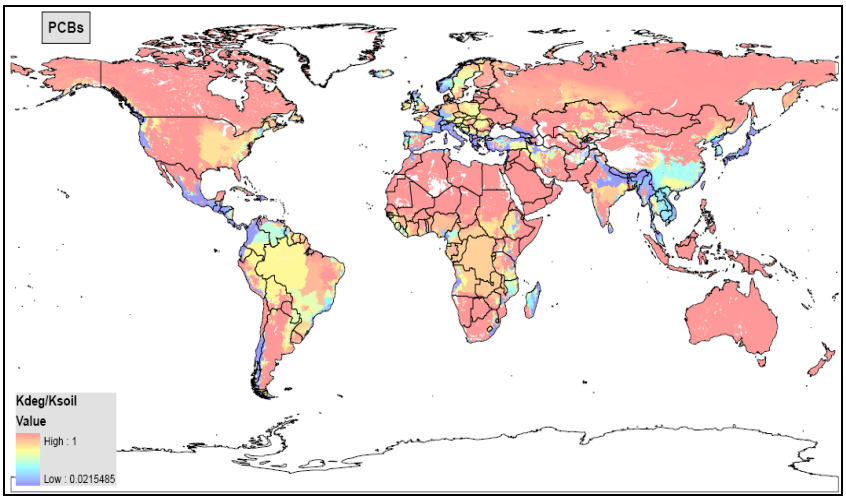

(b) - ratio of removal rate due to degradation to total Ksoil (global mean=0.97)

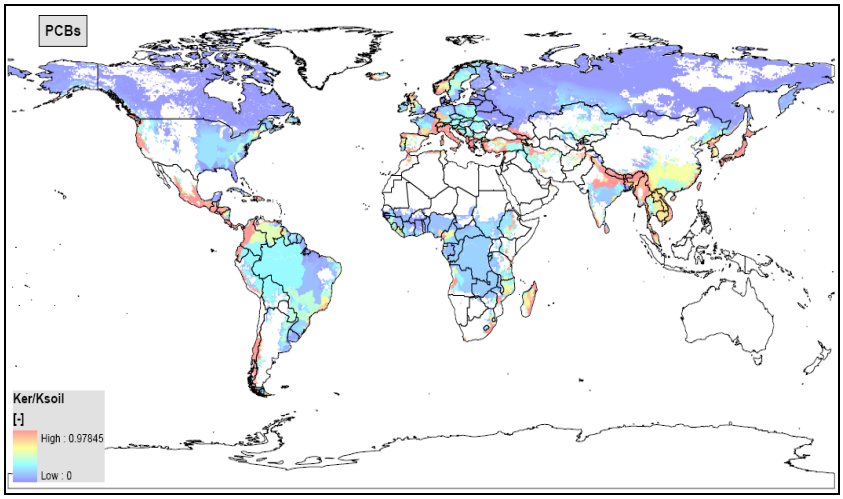

(c) - ratio of removal rate due to erosion to total Ksoil (global mean=0.025; std.dev.=0.06)

Figure 12 – Maps of soil removal rates of PCBs

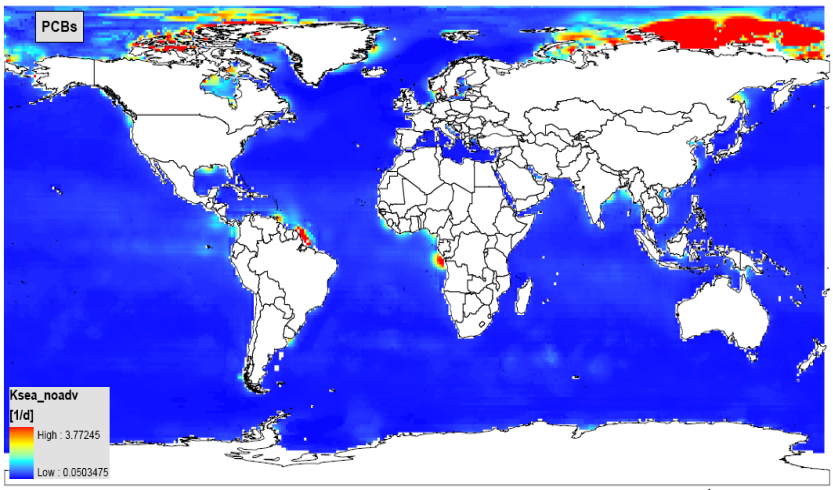

(a) - total ocean removal rate no advection (global mean=0.17 d^{-1}; std.dev.=0.11)

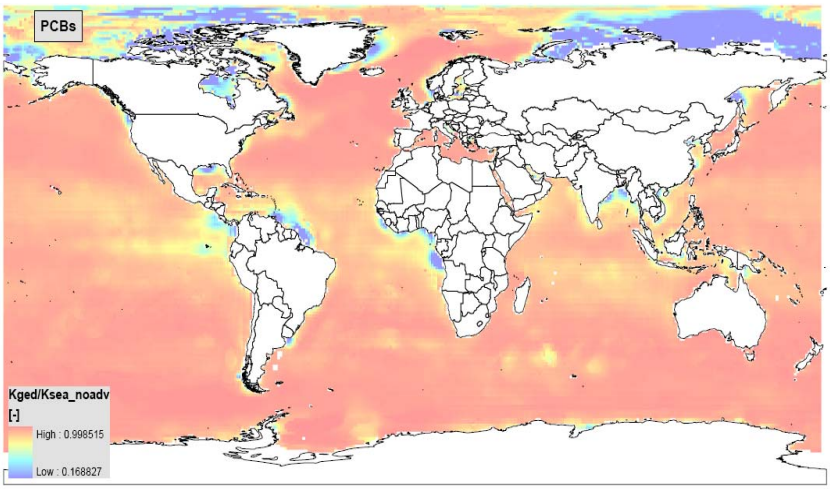

(b) - ratio of removal rate due to degradation to total Ksea_no adv (global mean=0.95)

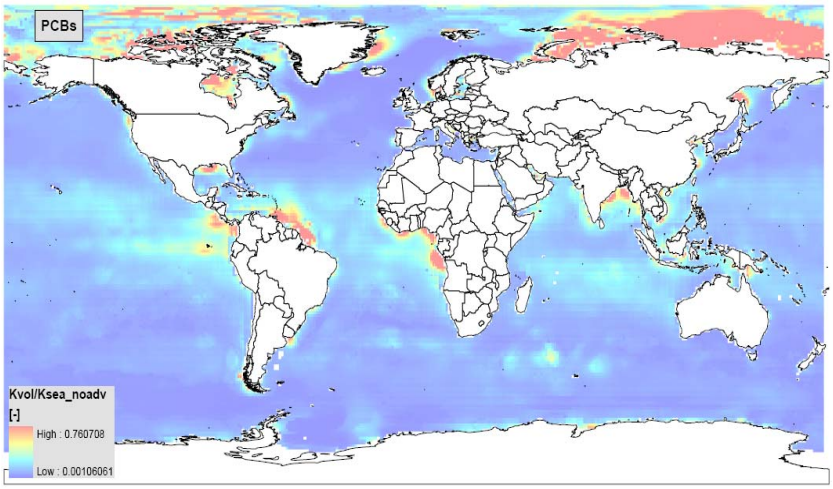

(c) - ratio of removal rate due to volatilisation to total Ksea_no adv (global mean=0.04; std.dev.=0.07)

Figure 13 - Maps of ocean removal rates of PCBs.

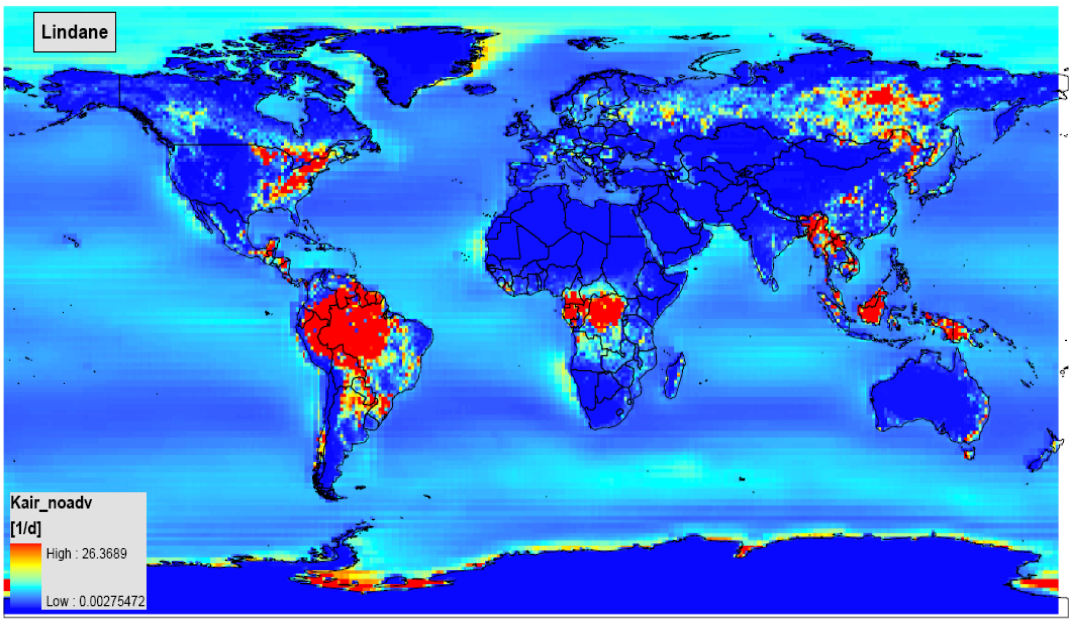

(a) - K'air no advection case (global mean=0.51 d^{-1}; std. dev.=0.91)

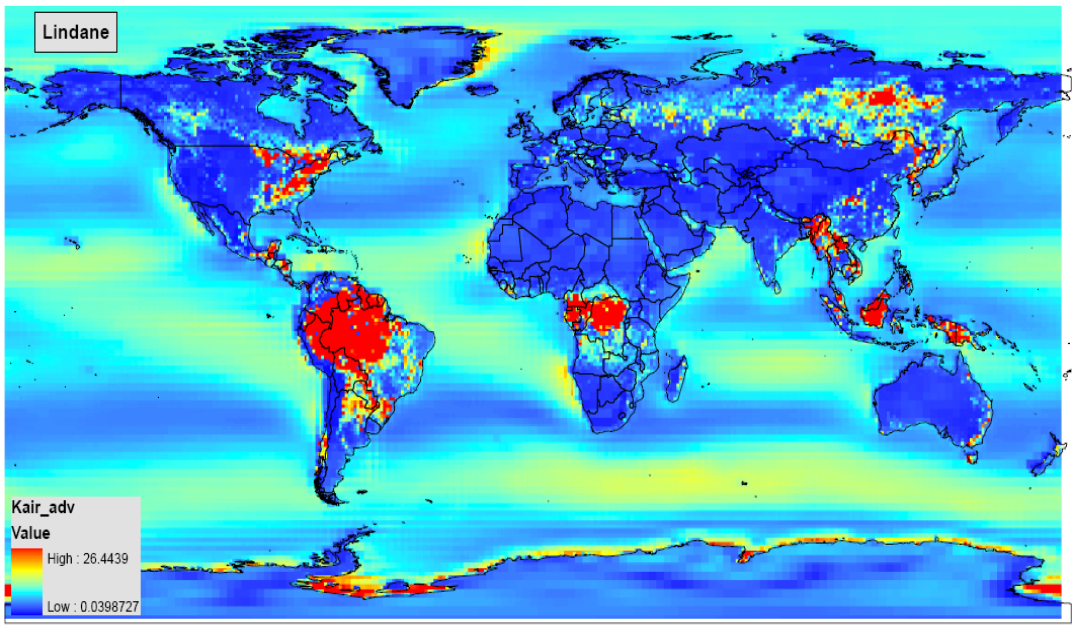

(b) - Kair advection case (global mean=0.84 d^{-1}; std. dev. =0.91)

Figure 14 - total air removal rates of Lindane.

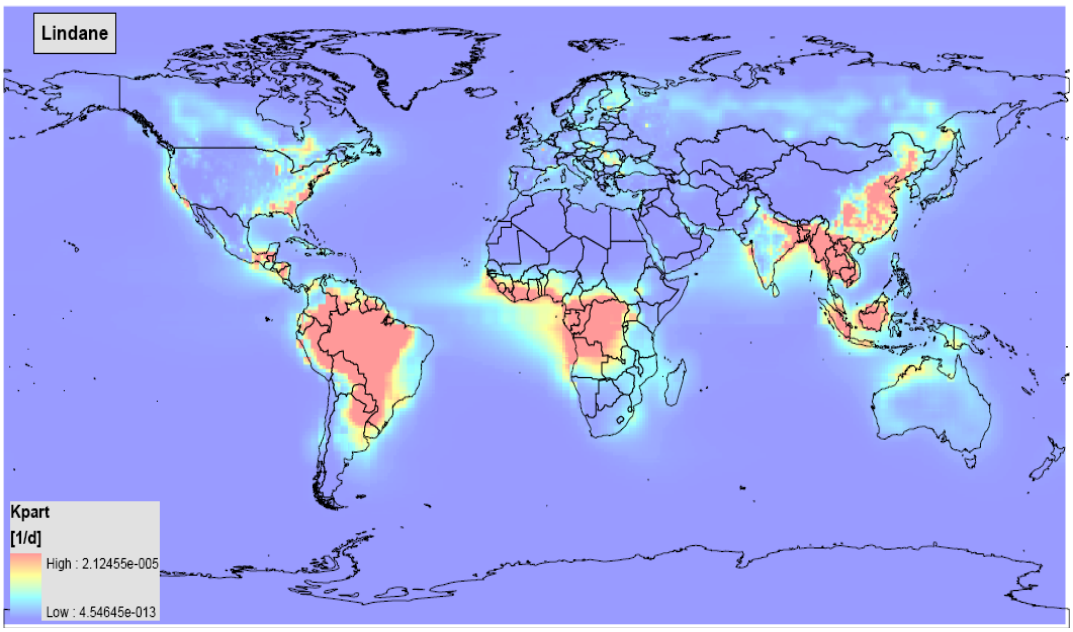

(a) - air removal rate due to particle deposition

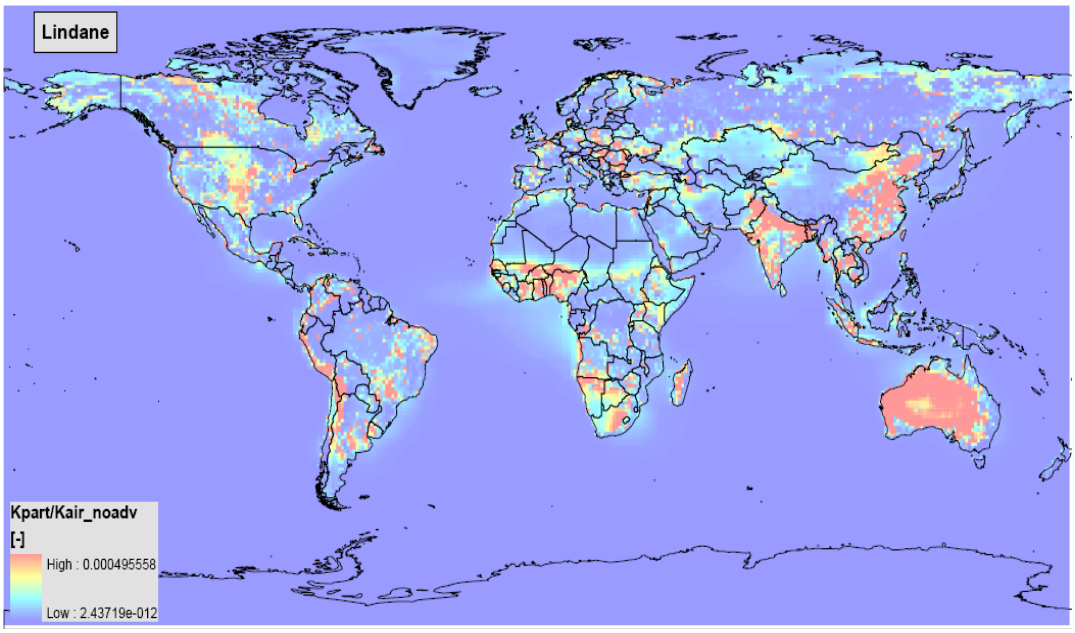

(b) - ratio of Kpart to K'air no advection (mean=2e-06)

Figure 15 – air particle dry deposition rate of Lindane.

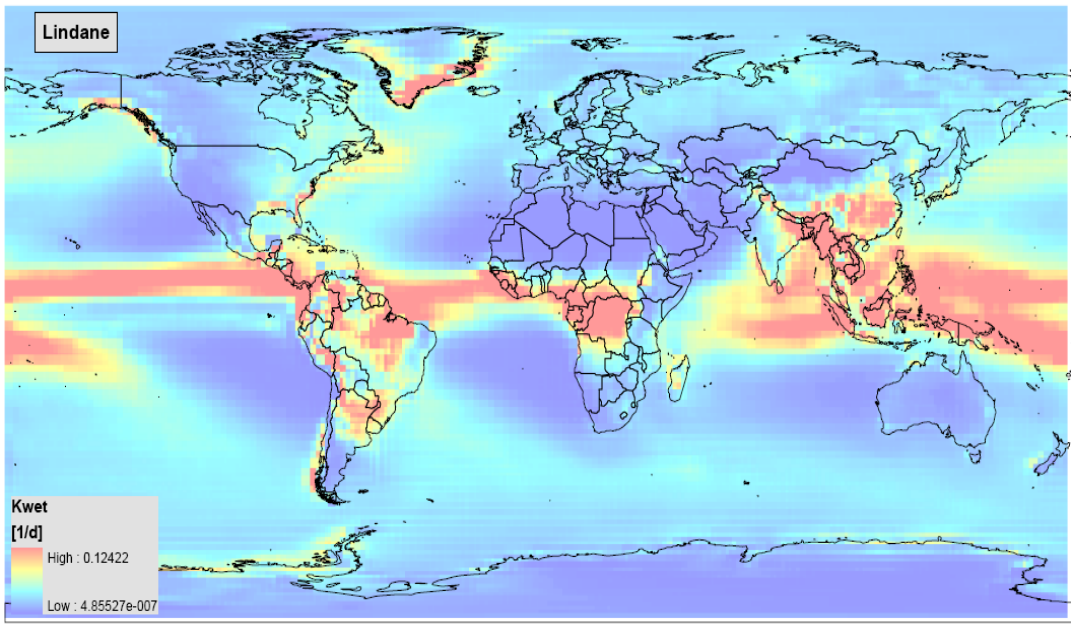

(a) - air removal rate due to wet deposition

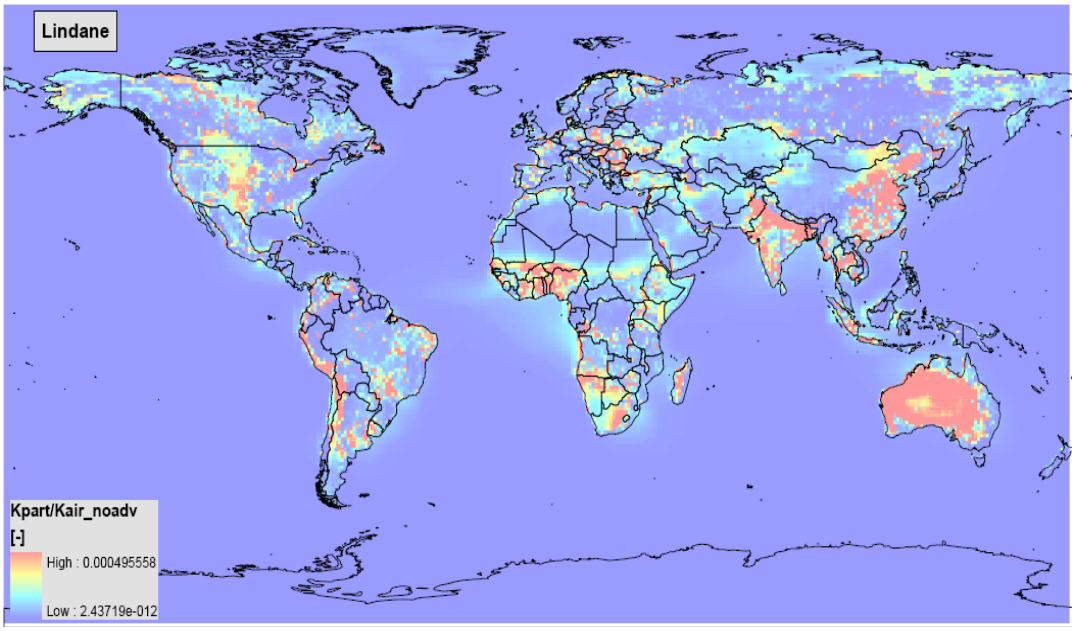

(b) - ratio of Kwet to K'air no advection (mean=0.047)

Figure 16 – air wet deposition rate of Lindane.

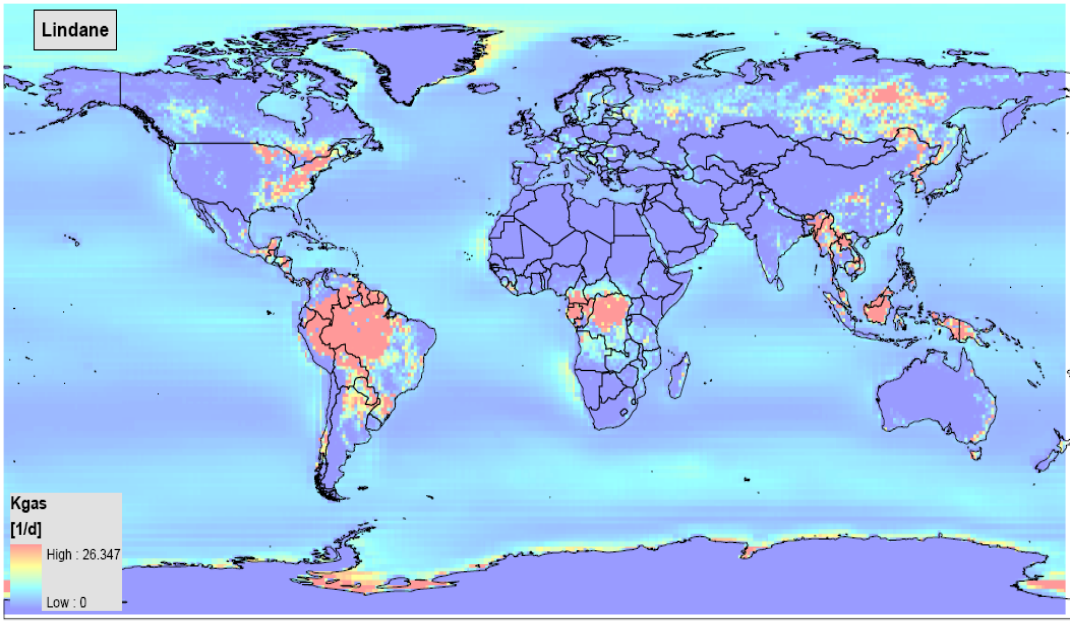

(a) - air removal rate due to gas exchange

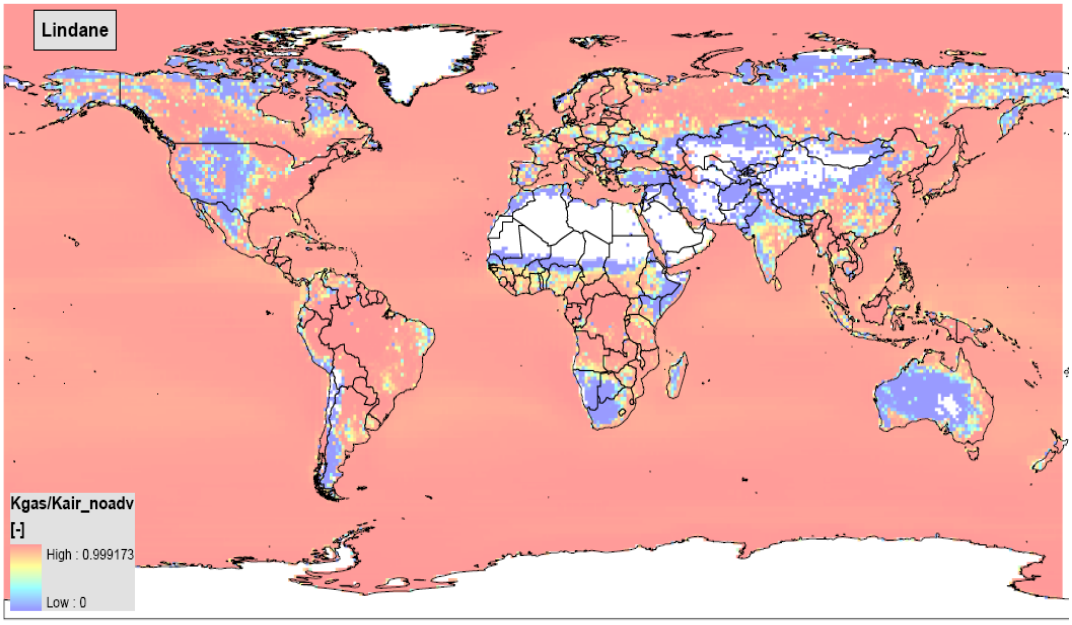

(b) - ratio of Kgas to K'air no advection (mean=0.773)

Figure 17 – air gas exchange rate of Lindane.

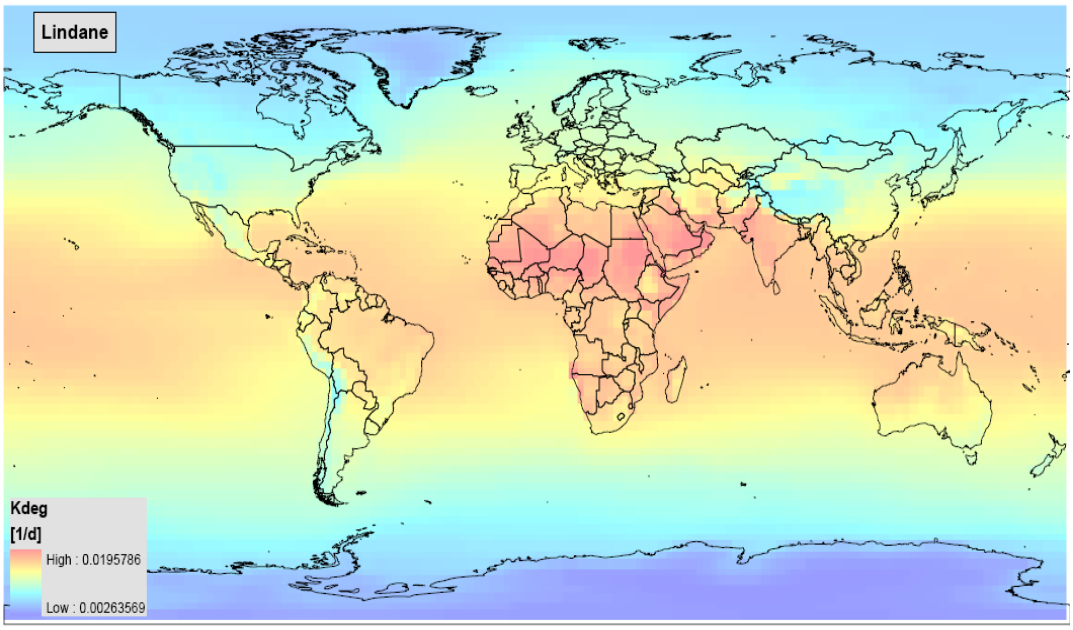

(a) - air removal rate due to degradation (temperature dependant)

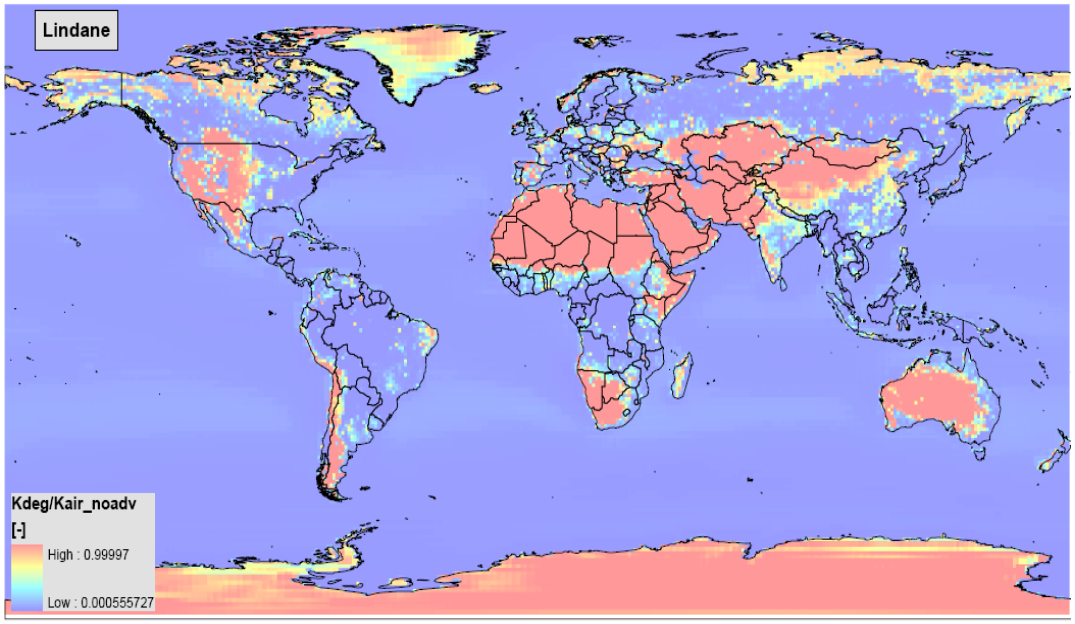

(b) - ratio of Kdeg to K'air no advection (mean=0.179)

Figure 18 - air degradation rate of Lindane.

6. Global non-spatial transient model

The section presents an example of how the maps of environmental removal rates, calculated by MAPPE Global model, could be further explored to feed and support the simulations by a global transient box model. This zero-dimensional time-dependent global model represents an alternative formulation of the MAPPE model, which is consistent with the spatialized MAPPE model but enables contaminant fate calculations.

The non-spatial (zero-dimensional) time-dependent global model is shortly described below. For each environmental compartment, it accounts a general mass balance equation in the form:

$$V\frac{dC}{dt} = emission - kCV$$

where C is concentration, V is the compartment bulk volume, "emission" includes direct emissions and transfer from other media, and k is the overall removal rate. For example, this conceptualization was used to develop Earth box model to quantify the timely trend of DDT in different environmental media for a period of few decades (Schenker et al, 2008) including a forecast up to 2050.

Then, the balance equation for the evaluative world is written in a matrix form as follows:

$$\begin{bmatrix} (E_a) \\ (E_L) \\ \left(E_O + E_w e^{-\frac{\ln 2}{DT_{50,w}}\tau_w}\right) \end{bmatrix} - \begin{bmatrix} (k_a + \frac{1}{\tau_a})ABL & -(k_{VL,L} f_L)\Delta & -(k_{VL,O} f_O)MLD \\ -k_{dep} f_L ABL & k_s \Delta & 0 \\ -k_{dep} f_O ABL & k_{RO}\Delta e^{-\frac{\ln 2}{DT_{50,w}}\tau_w} & (k_O + \frac{1}{\tau_O})MLD \end{bmatrix} \begin{bmatrix} c_a \\ c_L \\ c_O \end{bmatrix} = \frac{d}{dt}\begin{bmatrix} c_a \\ c_L \\ c_O \end{bmatrix}$$

In most cases, feedback loops may be neglected (Margni et al., 2004), therefore, the above differential equations may be decoupled and solved independently in a cascade mode.

Here the indexes *a, L, O, w* denote air, land, ocean and fresh water, respectively. The other symbols mean:

- E_i *(i=a, L, O, w)* represent the emission for each compartment
- k_i *(i=a, L, O)* represent the sum of rates of degradation, diffusive and vertical advection or the total removal rate.
- τ_i *(i=a, w, O)* represent retention times, i.e. the ratios of compartment fluid bulk volume over volumetric discharge through the volume boundary (not defined for the land compartment)
- $DT_{50,w}$ is the substance half-life in inland surface water
- k_{dep} is the total atmospheric deposition rate
- $k_{VL,L}$ and $k_{VL,O}$, are the volatilization rates from land and ocean, respectively;
- f_L and f_O are the fractions of the cell which are land and ocean, respectively
- *ABL* and *MLD* are the atmospheric boundary layer height and ocean mixing depth, respectively
- Δ is the soil layer thickness

Formerly, the maps of removal rates in air, ocean, soil and inland water estimated by the MAPPE Global model can be used to provide input to the non-spatial model described above, which in turn enables drawing a picture of the time trends of chemical fate at global scale, taking into account the spatial variability of environmental processes.

As an example application, we refer to the case of DDT, a long and thoroughly studied chemical for which a recent global model was developed by Schenker et al. (2008). These authors estimated physico-chemical properties and emissions of DDT over many years, and applied the CliMoChem model to predict temporal trends of ocean, soil and air concentrations for all latitudinal zones of the world. In the example presented here, we only refer to the global trends, but obviously the model may focus on specific zonal applications.

The modeling exercise starts from the emission estimates by Schenker et al. (2008), as per Figure 19.

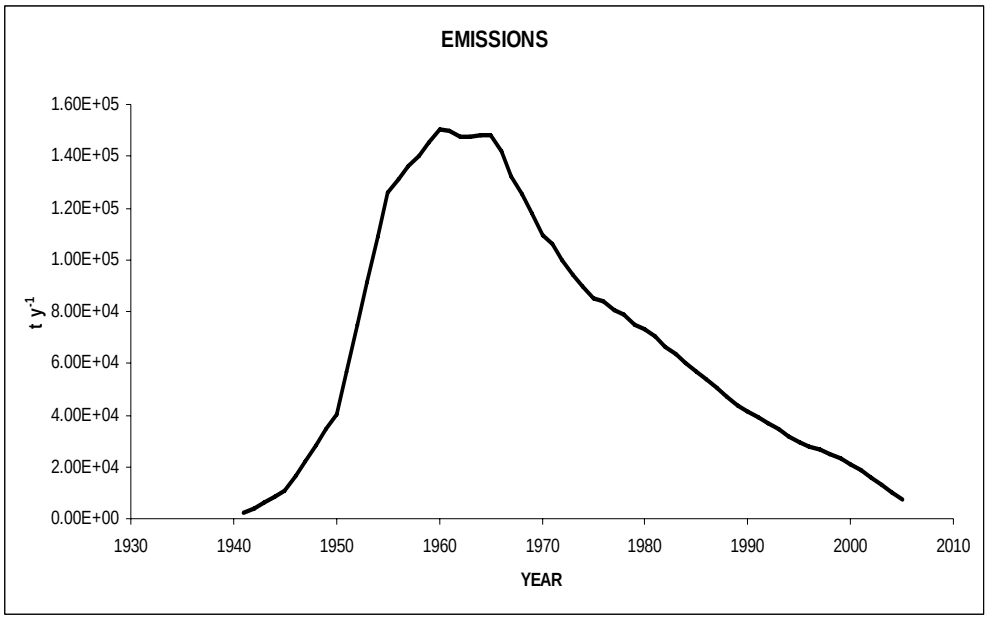

Figure 19 – global DDT emissions according to Schenker et al., (2008).

Formerly, we used the results of MAPPE Global model to find estimates of the atmospheric removal rates for DDT. These include advection, dry and wet deposition in gas and particulate phase, and degradation.

For degradation, we consider the Arrhenius equation with the same parameters suggested by Schenker et al. (2008) for soil, air and water, and we derive a simple exponential law of degradation rate as a function of temperature through nonlinear regressions (see Figure 20).

In a similar way the exponential law for air-water partition coefficient is found as presented on Figure 21. The octanol-water partition coefficient is assumed to be 2570395.78 as adopted in Schenker et al. (2008).

Then, from the maps for the different environmental removal rates, produced by MAPPE Global, we extract the 5^{th} , 95^{th} and 50^{th} percentiles (see Table 5). This enables to forecast the "median situation" and its variability in terms of 5 and 95% confidence intervals.

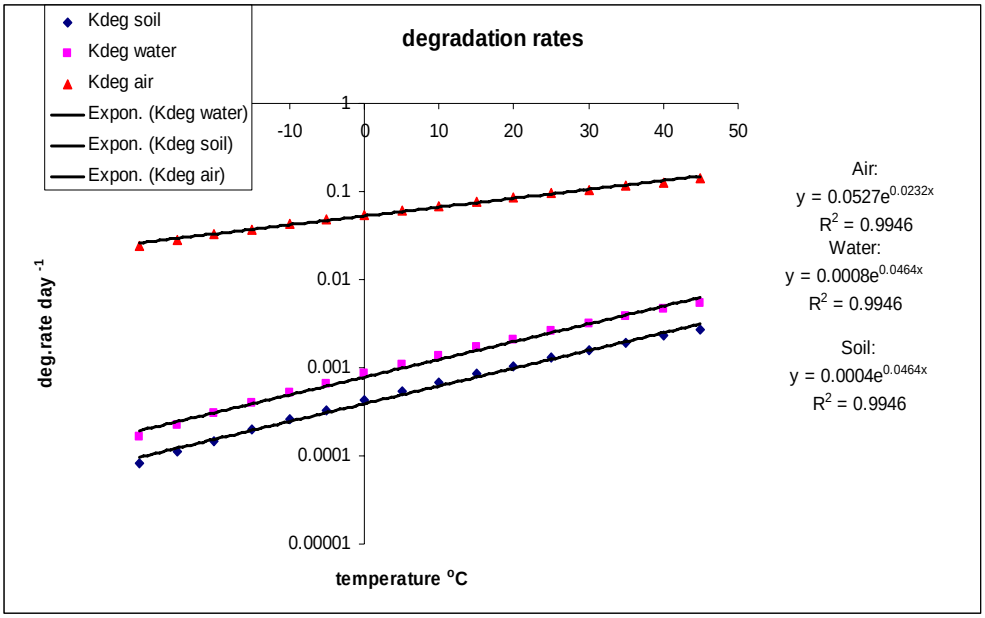

Figure 20 – estimation of degradation in air, water and soil

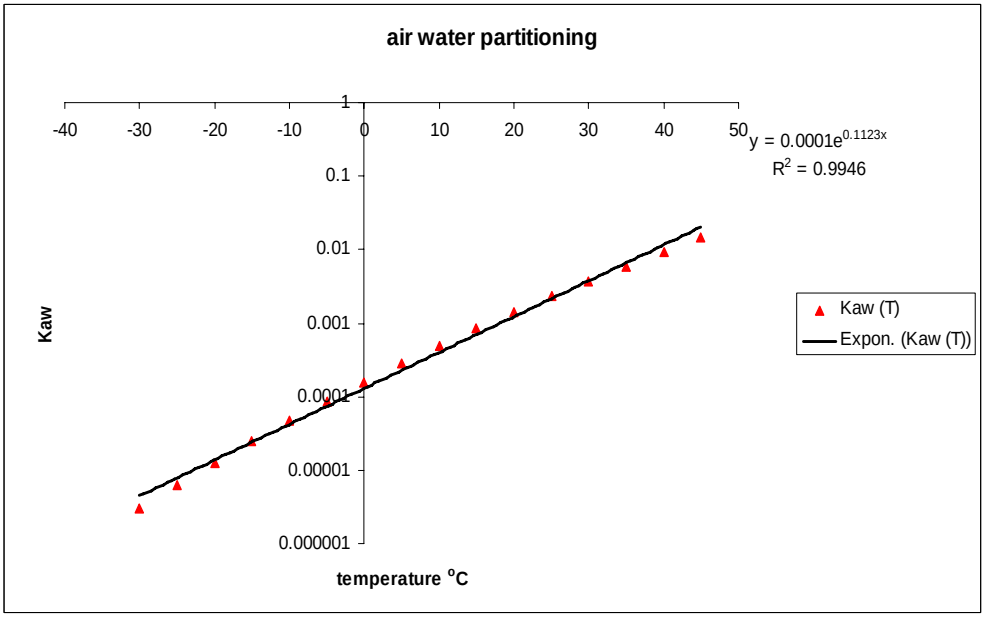

Figure 21 – estimation of degradation in air, water and soil

Removal rate	***5%ile***	***median***	***95%ile***
Air, overall	9.95E-02	4.01E-01	7.16E+00
Atmospheric deposition	3.23E-02	2.82E-01	7.06E+00
Soil, overall	2.93E-04	1.00E-03	4.21E-03
Soil, runoff+erosion	0.00E+00	1.07E-04	3.46E-03
Ocean, overall	3.09E-02	6.92E-02	1.86E-01
Ocean, overall (no advection)	1.57E-03	7.77E-03	4.98E-02

Table 5 – statistics of the environmental removal rates (units of day^{-1})

For instance, we then compute mass in air at the end of the generic year t as:

$$M(t) = M(t-1) \exp(-K \times 365) + E(t) \times (1 - \exp(-K \times 365)) / K$$

where E(t) is the emission of DDT to atmosphere during year t, M(t-1) is the mass of DDT at the end of year (t-1), and K is the overall removal rate in air.

Furthermore, the atmospheric deposition during year t, D(t), is given by:

$$D(t) = M(t) \times Kdep$$

where Kdep is the air deposition rate. We repeat the calculation using the time series of total emissions retrieved from Schenker et al.(2008), for the 5th, 95th and 50th percentiles of K and Kdep.

In calculations we assume that 20% of total emissions are to air, which is the upper extreme of the atmospheric emission share according to the authors. This enables computing a "median" M(t) and its 5-95% confidence interval. As a result, the approach accounts for the uncertainty that we have on atmospheric rates at global scale, if we do not consider the exact location of the DDT emission. The same applies for deposition; to compute the confidence interval, we considered only the deposition rates variability while we applied the median of the mass in atmosphere.

This type of calculations can be readily implemented in a spreadsheet and has no computational cost. The results for atmosphere are shown in Figure 22. It can be noticed immediately that the DDT mass has quite a large uncertainty due to neglecting spatial variation. On the other hand, the deposition is rather narrower. This is due to neglecting co-variation in mass and deposition, and to the lower spatial variability of deposition rates with respect to overall rates, also appreciably affected by degradation. It is also worth noting that, due to the relatively fast response of the air compartment to emissions (since higher removal rates) the series of emissions and masses or depositions show no appreciable time lag.

Similar calculations can be repeated for soils, lumping in the emission term both direct emissions to soils (80% of the total) and atmospheric deposition (assuming 40% of it occurs on land area). In this case, we compute the overall soil K and the sum of the erosion and runoff removal rates, which yield the load from soils to the stream network along the same logics used to compute deposition. Figure 23 shows the results, highlighting a generally lower uncertainty with respect to DDT mass in air, and a lag between the emission and mass time series. This is due to the generally lower soil removal rates, and is more apparent for the highest values of mass. The same, but less obviously, is observed for the loads to surface water.

The ocean compartment is treated in analogous way by adding to 60% of the atmospheric deposition the runoff and erosion loads and an additional 1% of total emissions, which represent direct emissions to water. In principle, the erosion and runoff loads should be reduced of a factor accounting for the retention of the chemical in the stream network. Given the long half-life of DDT in water, however, this has been neglected. Although the ocean removal rates are faster than the ones in soils, still no appreciable lag is highlighted between emission and mass time series (see Figure 24).

The non-spatial global box model results indicate that the peak of DDT mass in the different media occurs around 1965, relatively close to the peak of emissions. The time series we produce are well in line with the ones of Schenker et al. (2008). The calculations, presented here, however, cannot be used directly for a global mass balance of DDT as the different percentiles do not refer necessarily to the same locations. However, each individual time series represents reasonable ranges of variations of masses and fluxes in different media. In particular, if we convert mass time series into concentrations, we find a good agreement with the results of Schenker et al. (2008) (in particular, Figure 2 of that paper), which provides the trend of air, soil and ocean DDT concentrations in the period 1985-1995. Here the concentrations (see Figure 25) were derived from mass divided by the earth surface area (5.31×10^{14} m^2) and the average compartment depth considered in the model (air boundary layer: 641 m; soil depth: 0.3 m; ocean mixing depth: 58.5 m) assuming a proportion of 40% of land area and 60% of ocean area, which overestimates land but accounts for the proximity of emissions to land.

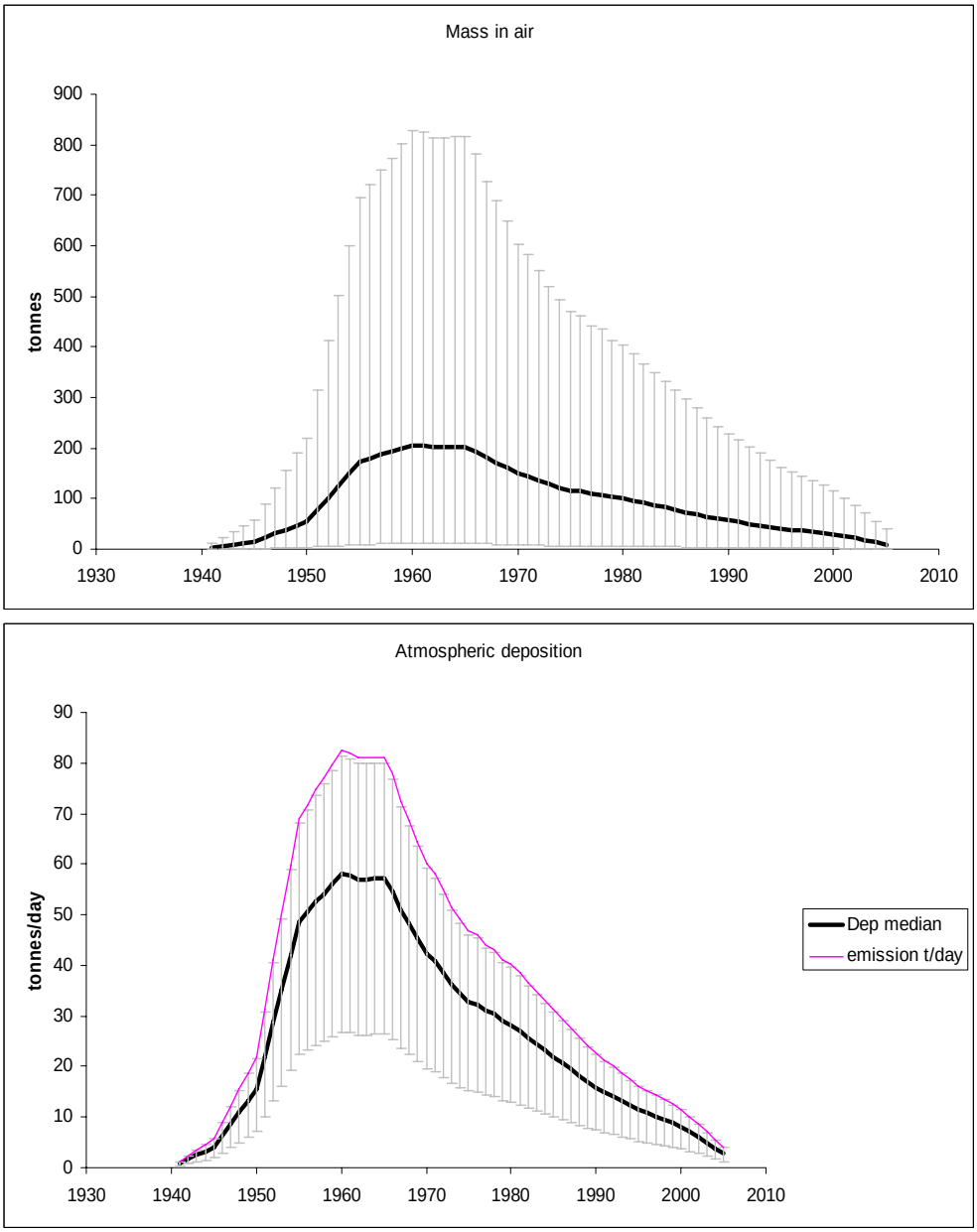

Figure 22 – DDT in air: mass (above); deposition (below)

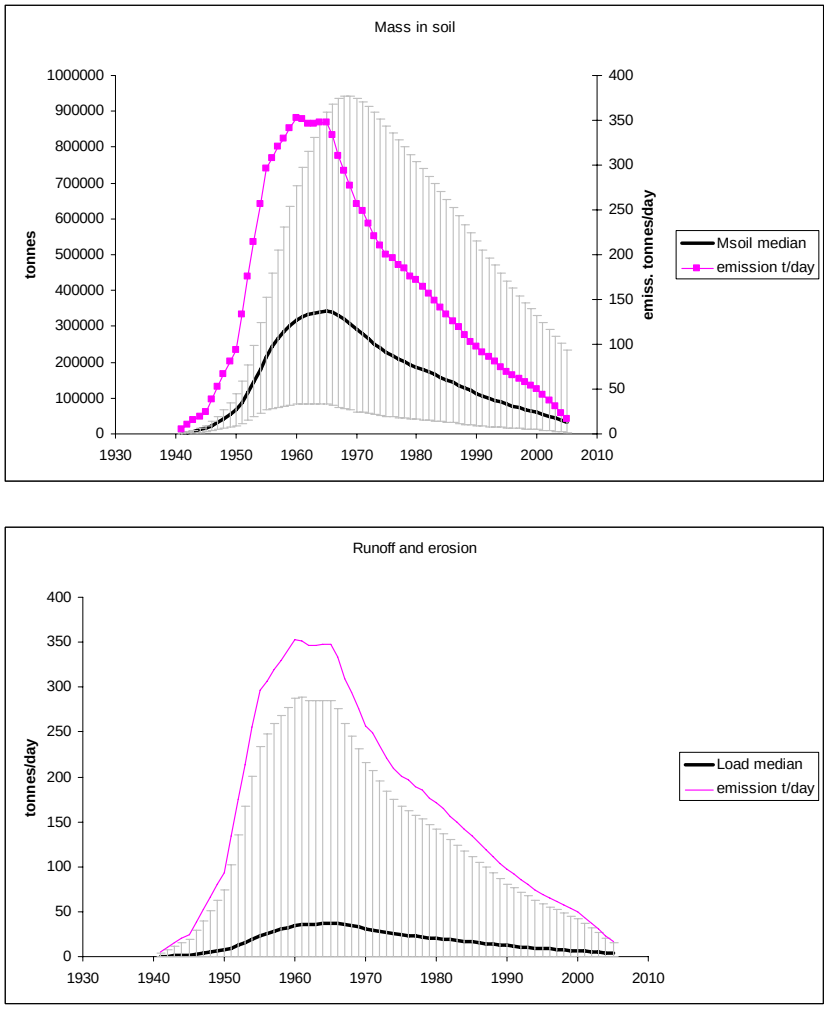

Figure 23 – DDT in soil: mass (above); load to the stream network (below).

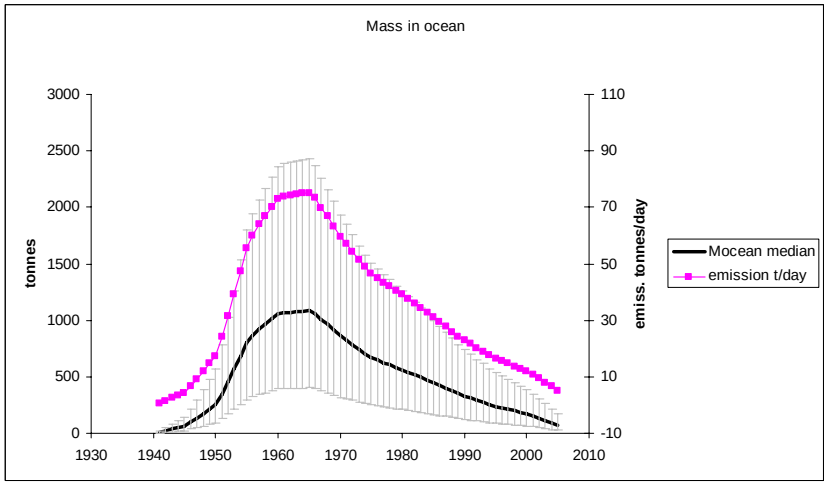

Figure 24 – DDT mass in ocean.

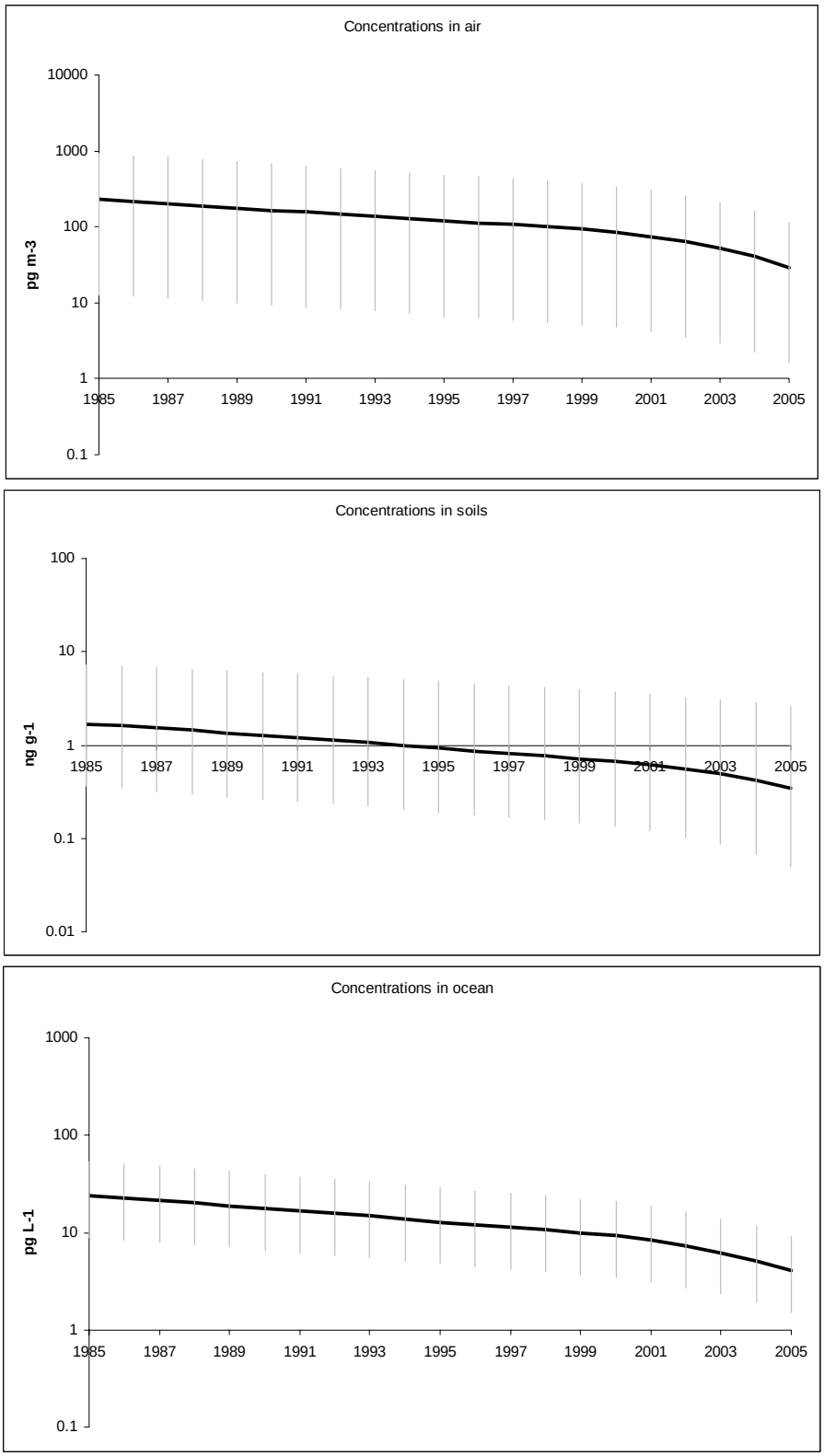

Figure 25 – concentrations in air, soil and ocean for 1985-1995 time period.

References

Baines, S.B., Pace, M.L., Karl, D.M., 1994. Why does the relationship between sinking flux and planktonic primary production differ between lakes and oceans? *Limnology and Oceanography*, vol. 39, n. 2, 213-226.

Dachs. J., R. Lohmann, W. Ockenden, L. Mejanelle, S.J Eisenreich, and K. Jones, 2002. Oceanic Biogeochemical Controls on Global Dynamics of Persistent Organic Pollutants**,** *Environmental Science and Technology,* v. 36, 4229-4237

Margni, M., D. W. Pennington, D. H. Bennett and O. Jolliet, 2004, Cyclic Exchanges and Level of Coupling between Environmental Media: Intermedia Feedback in Multimedia Fate Models, *Environmental Science and Technology*, v. 38, 5450-5457

Legendre,L., Michaud, J., 1999. Chlorophyll a to estimate the particulate organic carbon available as food to large zooplankton in the euphotic zone of oceans, *Journal of Plankton research*, vol. 21, no. 11, pp 2067-2083

McLachlan, M., Horstmann, M., 1998. Forests as filters of airborne organic pollutants: a model, *Environmental Science and Technology*, v. 32, 413-420

Pennington, D.W., M. Margni, Ch. Ammann, and O. Jolliet, 2005, Multimedia Fate and Human Intake Modeling: Spatial versus Nonspatial Insights for Chemical Emissions in Western Europe, *Environ. Sci. Technol.*, *39* (4), 1119–1128

Pistocchi, A., 2008. A GIS-based approach for modeling the fate and transport of pollutants in Europe, *Environmental Science and Technology*, 42, 3640-3647.

Pistocchi, A., 2005. Report on multimedia fate and exposure model with various spatial resolutions at the European level, *NoMiracle IP D2.4.1 technical report*, 62 pp

Pistocchi, A., D.A. Sarigiannis, P. Vizcaino, 2010a. Spatially explicit multimedia fate models for pollutants in Europe: State of the art and perspectives, *Science of the Total Environment*, Volume 408, Issue 18*,* 3817-3830

Pistocchi, A., G. Zulian, P. Vizcaino, D. Marinov, 2010b. Multimedia Assessment of Pollutant Pathways in the Environment, European scale model (MAPPE EUROPE). *JRC Scientific and Technical Reports, EUR 24256 EN*, Office for Official Publications of the European Communities, Luxembourg: 53 pp.

Rosenbaum RK, Bachmann TM, Gold LS, Huijbregts MAJ, Jolliet O, Juraske R, Köhler A, Larsen HF, MacLeod M, Margni M, McKone TE, Payet J, Schuhmacher M, van de Meent D, Hauschild MZ, 2008. USEtox - The UNEP-SETAC toxicity model: recommended characterization factors for human toxicity and freshwater ecotoxicity in Life Cycle Impact Assessment. *Int. J. LCA*, 13(7):532-546

Sala, S., D. Marinov, D. Pennington, 2011. Spatial differentiation of chemical removal rates from air in Life Cycle Impact Assessment, *Int. J. LCA,* doi: 10.1007/s11367-011-0312-8

Shaked S, Friot D, Humbert S, Margni M, Schwarzer S, Wannaz C, 2008, Health impacts of trade: integration of multimedia multi-continental model and a global input–output trade model. Pasadena CA, USA: ISEA.

Schwarzenbach, R. P.; Gschwend, P. M.; Imboden, D. M., 1993. Environmental Organic Chemistry; Wiley: New York, 681pp.

Zulian, G., P. Isoardi, A. Pistocchi, 2010, Global atlas of environmental parameters for chemical fate and transport assessment, *JRC Scientific and Technical Reports, EUR 24255 EN*, Office for Official Publications of the European Communities, Luxembourg: 80 pp.

European Commission

EUR 24911 EN – Joint Research Centre – Institute for Environment and Sustainability
Title: Multimedia assessment of pollutant pathways in the environment: a Global scale model
Author(s): A. Pistocchi, D. Marinov, S. Pontes, G. Zulian, M. Trombetti

Luxembourg: Publications Office of the European Union
2011 – 50 pp. – 21 x 29.7 cm
EUR – Scientific and Technical Research series - ISSN 1018-5593 (print), ISSN 1831-9424 (online)

ISBN 978-92-79-20921-5 (print)
ISBN 978-92-79-20922-2 (pdf)

doi: 10.2788/47157

Abstract
The report describes the assumptions, equations and a few examples of preliminary applications of a global spatial steady-state box model entitled Multimedia Assessment of Pollutant Pathways in the Environment (MAPPE-Global). The model grounds on the concept of already developed European version of MAPPE chemical fate model.

MAPPE-Global computes the removal rates of a substance with given physical-chemical properties in an evaluative environment for the Globe with a resolution of 1^{o}x1^{o} considering atmosphere, land (natural and agriculture soils, forests, impervious surfaces, frozen territories), surface water (including lakes, inland wetlands and reservoirs) and oceans and seas.

MAPPE-Global is able to consider chemical emissions in one or more of the environmental compartments and estimates chemical concentrations and fluxes accounting chemical partitioning (gas, liquid or solid), degradation, advective and diffusive transport.

At this stage, MAPPE Global does not explicitly compute chemical transport in space, but only the fate of a substance at each location in space. However, the model estimates for each grid cell the mass fluxes of chemical that are available for transport inside or outside of the cell, in addition to concentrations from local emissions. Thus, MAPPE Global is developed specifically to respond questions as:

- How will a chemical spread across different media in the different climatic and landscape settings?
- How important is the variability of environmental processes in determining the fate of chemicals across the globe?

In addition, the model enables estimating, for virtually any location in the world, representative parameters of the environmental removal rates that determine the fate of a contaminant. These rates may be used to feed a zero-dimensional time-dependent model that allows computing the main receptors of the chemical emissions.

Besides, in order to evaluate the performance of the MAPPE-Global model a comparison with established models, such as Impact World and USEtox was made by crosschecking of the intermedia removal rate coefficients.

Finally, MAPPE-Global was used to quantify for a set of 34 representative pollutants at global scale the range of variability of chemical removal rates for the different environmental compartments and to identify the fate patterns of flyers, swimmers, soil-bound and multimedia chemical substances.

How to obtain EU publications

Our priced publications are available from EU Bookshop (http://bookshop.europa.eu), where you can place an order with the sales agent of your choice.

The Publications Office has a worldwide network of sales agents. You can obtain their contact details by sending a fax to (352) 29 29-42758.

The mission of the JRC is to provide customer-driven scientific and technical support for the conception, development, implementation and monitoring of EU policies. As a service of the European Commission, the JRC functions as a reference centre of science and technology for the Union. Close to the policy-making process, it serves the common interest of the Member States, while being independent of special interests, whether private or national.

JRC
EUROPEAN COMMISSION

LB-NA-24911-EN-C

Publications Office

ISBN 978-92-79-20921-5